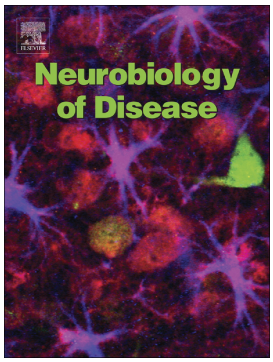

The lysosomal enzyme alpha-Galactosidase A is deficient in Parkinson's disease brain in association with the pathologic accumulation of alpha-synuclein

Michael P. Nelson, Michel Boutin, Tonia E. Tse, Hailin Lu, Emily D. Haley, Xiaosen Ouyang, Jianhua Zhang, Christiane Auray-Blais, John J. Shacka

PII: S0969-9961(17)30272-3
DOI: doi:10.1016/j.nbd.2017.11.006
Reference: YNBDI 4061

To appear in: *Neurobiology of Disease*

Received date: 25 August 2017
Revised date: 17 November 2017
Accepted date: 27 November 2017

Please cite this article as: Michael P. Nelson, Michel Boutin, Tonia E. Tse, Hailin Lu, Emily D. Haley, Xiaosen Ouyang, Jianhua Zhang, Christiane Auray-Blais, John J. Shacka , The lysosomal enzyme alpha-Galactosidase A is deficient in Parkinson's disease brain in association with the pathologic accumulation of alpha-synuclein. The address for the corresponding author was captured as affiliation for all authors. Please check if appropriate. Ynbdi(2017), doi:10.1016/j.nbd.2017.11.006

The lysosomal enzyme alpha-Galactosidase A is deficient in Parkinson's disease brain in association with the pathologic accumulation of alpha-synuclein

Michael P. Nelson[1], Michel Boutin[2], Tonia E. Tse[1,3], Hailin Lu[1], Emily D. Haley[1,3], Xiaosen Ouyang[1], Jianhua Zhang[1,4], Christiane Auray-Blais[2] and John J. Shacka[1,3,4,5]

[1]Dept. Pathology, University of Alabama at Birmingham, Birmingham, AL

[2]Division of Medical Genetics, Department of Pediatrics, Centre de Recherche-CHUS, Faculty of Medicine and Health Sciences, Université de Sherbrooke, Sherbrooke, Quebec, Canada

[3]Dept. Pharmacology & Toxicology, University of Alabama at Birmingham, Birmingham, AL

[4]Birmingham VA Medical Center, Birmingham, Alabama

[5]Corresponding Author

Dept. Pharmacology & Toxicology, University of Alabama at Birmingham 1670 University Blvd, VH 257, Birmingham, AL 35294

ABSTRACT

The aberrant accumulation of alpha-synuclein (α-syn) is believed to contribute to the onset and pathogenesis of Parkinson's disease (PD). The autophagy-lysosome pathway (ALP) is responsible for the high capacity clearance of α-syn. ALP dysfunction is documented in PD and pre-clinical evidence suggests that inhibiting the ALP promotes the pathological accumulation of α-syn. We previously identified the pathological accumulation of α-syn in the brains of mice deficient for the soluble lysosomal enzyme alpha-Galactosidase A (α-Gal A), a member of the glycosphingolipid metabolism pathway. In the present study, we quantified α-Gal A activity and levels of its glycosphingolipid metabolites in postmortem temporal cortex specimens from control individuals and in PD individuals staged with respect to α-syn containing Lewy body pathology. In late-state PD temporal cortex we observed significant decreases in α-Gal A activity and the 46 kilodalton "active" species of α-Gal A as determined respectively by fluorometric activity assay and western blot analysis. These decreases in α-Gal A activity/levels correlated significantly with increased α-syn phosphorylated at serine 129 (p129S-α-syn) that was maximal in late-stage PD temporal cortex. Mass spectrometric analysis of 29 different isoforms of globotriaosylceramide (Gb_3), a substrate of α-Gal A indicated no significant differences with respect to different stages of PD temporal cortex. However, significant correlations were observed between increased levels of several Gb_3 isoforms and with decreased α-Gal A activity and/or increased p129S-α-syn. Deacylated Gb_3 (globotriaosylsphingosine or lyso-Gb_3) was also analyzed in PD brain tissue but was below the limit of detection of 20 pmol/g. Analysis of other lysosomal enzymes revealed a significant decrease in activity for the lysosomal aspartic acid protease cathepsin D but not for glucocerebrosidase (GCase) or cathepsin B in late-stage PD temporal cortex. However, a significant correlation was observed between decreasing GCase activity and increasing p129S-α-syn. Together our findings indicate α-Gal A deficiency in late-stage PD brain that correlates significantly with the pathological accumulation of α-syn, and further suggest the potential for α-Gal A and its glycosphingolipid substrates as putative biomarkers for PD.

KEYWORDS

Alpha-Galactosidase A; alpha-synuclein; globotriaosylceramide; glycosphingolipids; Parkinson's disease; lysosome

ABBREVIATIONS

4-Methylumbelliferone α-D-galactopyranoside (4-MUG); N-Acetyl-D-galactosamine (GalNAc); alpha-Galactosidase A (α-Gal A); alpha-synuclein (α-syn); autophagy-lysosome pathway (ALP); cathepsin B (Cat B); cathepsin D (Cat D); globotriaosylceramide (Gb_3); globotriaosylsphingosine (lyso-Gb_3); glucocerebrosidase (GCase); incidental Lewy body disease (ILBD); kilodalton (kDa); lysosome-associated membrane protein-2 (LAMP-2); Parkinson's disease (PD); p129S-α-syn (alpha-synuclein phosphorylated at serine 129); sphingomyelin (SM)

INTRODUCTION

Parkinson's disease (PD) is defined by substantia nigra neuron loss in addition to the pathologic accumulation of α-syn-containing Lewy body inclusions and neurites (Spillantini et al. 1997). Alpha-synuclein (α-syn) pathology correlates temporally and spatially with PD progression as it is typically limited to lower brain regions in early disease prior to its later spread to motor and cognitive centers (Beach et al. 2009; Braak et al. 2003). While α-syn is ordinarily a soluble, natively unfolded monomer, a multi-step *in vitro* process of its folding and oligomerization produces insoluble fibrils similar to those present in PD brain (Conway et al. 2000). Moreover, α-syn mutations and replications in familial PD support its causal role for PD pathogenesis (Polymeropoulos et al. 1997; Singleton et al. 2003). Although it is still unclear how α-syn regulates PD pathogenesis, ample pre-clinical evidence indicates the neurotoxic potential of α-syn (Danzer et al. 2012, 2007; Desplats et al. 2009; Lee et al. 2013; Luk et al 2012, 2009; Volpicelli-Daley et al. 2011). The high-capacity clearance of α-syn is regulated by the ALP (reviewed in Shacka et al. 2008) and its function is compromised in normal aging brain and PD brain (Anglade et al. 1997; Cook et al. 2012; Dehay et al. 2012, 2010; Mazzulli et al. 2011; Zhu et al. 2003). Alpha-syn accumulation and toxicity are exacerbated by experimental inhibition of the ALP and attenuated by ALP induction (Danzer et al. 2012; Dehay et al. 2010; Klucken et al. 2012; Lee et al. 2013, 2004; Mader et al. 2012; Mangieri et al. 2014; Mazzulli et al. 2011; Pivtoraiko et al. 2010; Qiao et al. 2008; Sarkar et al. 2007). Conversely, it has also been shown that excess α-syn inhibits the ALP (Mazzulli et al. 2011; Song et al. 2014; Winslow et al. 2010; Yap et al. 2013). Together these findings underscore a continued need to study the ALP in hopes of better understanding the pathogenesis and treatment of PD.

Studies suggest the glycosphingolipid metabolism pathway, with coordinate regulation of several lysosomal enzymes, is useful for identifying therapeutic targets for PD (Sybertz and Krainc, 2014). Glucocerebrosidase (GCase), a soluble lysosomal enzyme that is mutated in the lysosomal storage disorder Gaucher disease has received particular focus for its role in PD pathogenesis and therapy. Large-scale epidemiologic studies have identified mutations for the human *GBA1* gene that encodes GCase as PD risk factors (Lwin et al. 2004; Xu et al. 2010). Previous studies have indicated reductions in GCase activity in PD brain in association with the pathogenic accumulation of α-syn (Gegg et al. 2012; Mazzulli et al. 2011; Murphy et al. 2014), and results of preclinical studies suggest the utility of GCase as a therapeutic target for PD (Cullen et al. 2011; Mazzulli et al. 2011; Richter et al. 2014; Rocha et al. 2015; Sardi et al. 2013; Sybertz and Krainc, 2014; Wustman et al. 2014). Our previous analysis of PD brain tissues revealed no significant differences between stage of PD and levels of glucosylceramide

(substrate of GCase) (Boutin et al. 2016), which is in agreement with results from a previous study (Gegg et al. 2015). However, the known role for GCase deficiency in PD suggests that prospective analyses of glycosphingolipids could bolster their utility as putative PD biomarkers.

Alpha-Galactosidase A (α-Gal A) is a soluble lysosomal enzyme that is also in the glycosphingolipid pathway. Mutations in *GLA*, the human gene for α-Gal A cause the rare lysosomal storage disorder Fabry disease, a vasculopathy characterized pathologically by the dramatic accumulation of glycosphingolipids including globotriaosylceramide (Gb_3) and globotriaosylsphingosine (lyso-Gb_3) (Brady, 1967). We recently published a novel link between α-Gal A deficiency and α-syn accumulation as demonstrated by the pathologic accumulation of α-syn concomitant with disruption of ALP markers in α-Gal A-deficient mouse brains (Nelson et al. 2014). While it is unknown if Fabry patient brains harbor α-syn pathology, neuropathology has been documented in motor and non-motor brain regions affected by PD (de Veber et al. 1992; Kaye et al. 1988; Sung et al. 1975). Fabry patients have been diagnosed with extrapyramidal symptoms of Parkinsonism (Borsini et al. 2002; Buechner et al. 2006), demonstrating a putative connection between these two diseases. In addition, a polymorphism for *GLA* has been reported in a PD patient that may compromise its gene expression (Wu et al. 2002). However, whether α-Gal A levels and activity, and the glycosphingolipids metabolized by α-Gal A are altered in PD brain have not previously been investigated. Thus the goal of this study was to examine α-Gal A enzymatic activity and levels of glycosphingolipids metabolized by α-Gal A in post-mortem PD brain with respect to the pathologic accumulation of α-syn.

MATERIALS & METHODS

Cases. Human brain tissue samples of temporal cortex used in this study were obtained from the Banner Sun Health Research Institute Brain and Body Donation Program (Beach et al. 2008) following approval of our study and after receiving institutional review board ethics approval. Cases were staged with respect to α-syn-positive Lewy body pathology (Beach et al. 2009). Cases were selected to include neurologically normal controls without Lewy body disease (Stage 0, n = 12), and a range of cases from Stage IIa PD (Lewy pathology predominantly in olfactory bulb and brainstem, n = 6), Stage III PD (Lewy pathology in olfactory bulb, brainstem and limbic regions, n = 10) and Stage IV PD (significant Lewy pathology extended into neocortex, n = 10) as previously reported (Beach et al. 2009; Walker et al. 2013). Due to the relative lack of Stage IIa cases available for our study, incidental Lewy body disease (ILBD) cases (n = 6) were also included in our study. Lewy body pathology in the ILBD cases was limited to the olfactory bulb and brainstem, similar to that of Stage IIa PD (Beach et al.

2009); thus, Stage IIa PD and ILBD cases were combined as one group for experimental analyses. Four cases of PD were identified as having mutations in *GBA1* (personal communication, Thomas Beach, Banner Sun Health Institute): two Stage III cases (heterozygous for T369M or E326K), and two Stage IV cases (homozygous for N370S and compound heterozygous for T369M and V447). Other considerations for the selection of cases included sex distribution, age at death, postmortem interval and for PD cases, duration of disease (see **Table 1**). Upon receipt of brain specimens to the Shacka lab they were immediately stored at -80^{o}C until further processed. All brain specimens were cut into smaller pieces over dry ice. Representative samples from each case were subsequently shipped to the Auray-Blais lab for analysis of glycosphingolipids, or were transferred to the Zhang lab (at UAB for analysis of cathepsin B (Cat B) and cathepsin D (Cat D) enzymatic activity. Frozen whole brains from adult wild type and α-Gal A-deficient mice (Nelson et al. 2014) were also shipped to the Auray-Blais lab and served as controls for mass spectrometric analyses. Experiments with mice were performed in strict accordance to NIH guidelines for the care and use of laboratory animals, and with approval from the UAB Institutional Animal Care and Use Committee.

Brain processing for biochemical analyses. Fifty mg pieces of brain tissue were processed in a citrate-phosphate buffer (27 mM citrate and 46 mM disodium phosphate, pH 4.6) containing 1% Triton X-100 (Sigma), 1% protease inhibitor cocktail (Sigma P8340) and 1% of two different phosphatase inhibitor cocktails (Sigma P0044 and P5726) using a Dounce-type glass homogenizer. Homogenates were centrifuged @ 15,000 x *g* for 15 min, 4°C. Supernatants were aliquoted into fresh tubes for use in enzymatic activity assays for α-Gal A and GCase or for western blot analysis (as described below). For analysis of Cat D activity, brain tissues were lysed in buffer containing 50 mM Tris pH 7.4, 175 mM NaCl and 5 mM EDTA pH 8.0. These lysates were centrifuged @ 10,000 x *g* for 15 min, 4°C, with supernatants collected for analysis of activity. All protein homogenates were quantified using BCA protein assay (Thermo).

Western blot analysis. Western blot analysis was performed as described previously in our laboratory (Mangieri et al. 2014). In brief, brain homogenates were diluted in Laemmli sample buffer and heated at 90°C for 5 min. Equal amounts of homogenates were electrophoresed via SDS-polyacrylamide gel electrophoresis and subsequently transferred to PVDF membranes (Bio-Rad, Hercules, CA). Homogenates representing two cases from each group were run on each gel. Blots were probed with the following antibodies: rabbit anti alpha-syn phosphorylated at serine 129 (p129S-α-syn; Abcam ab168381); mouse anti-total α-syn (BD Biosciences BDB610787); rabbit anti-human α-Gal A (Genetex GTX101178); or mouse anti-

human LAMP-2 (Univ. Iowa Hybridoma Bank H4B4). Following incubation with HRP-conjugated anti-mouse or anti-rabbit secondary antibodies (BioRad) blots were developed using ECL western blotting substrate (Thermo). Blots were subsequently stripped and re-probed to control for loading using mouse anti-Actin (Sigma A1978). X-ray films of western blots were scanned for densitometric analysis using UN-SCAN-IT gel 6.1 software (Orem, UT).

Alpha-Gal A activity assay. Alpha-Gal A activity was measured using modifications of previously published protocols (Benjamin et al. 2009; Khanna et al. 2010). Brain homogenates were further diluted with substrate buffer containing 6 mM 4-Methylumbelliferone α-D-galactopyranoside (4-MUG; Sigma) and 90 mM N-Acetyl-D-galactosamine (GalNAc; Sigma). 4-MUG is cleaved to 4-MU by active α-Gal A whereas GalNAc is added to inhibit non-specific cleavage of 4-MUG by α-Galactosidase B (Beutler and Kuhl 1972). Triplicate wells of each sample were incubated for 1 h at 37°C, followed by the addition of stop buffer (0.4 M glycine, pH 10.8) and fluorescence measurement of 4-MU cleavage product at 460 nm. 4-MU fluorescence was quantified using a 4-MU standard curve performed for each assay. Activity was expressed as nmol 4-MU substrate/mg protein in sample/hour.

Glucocerebrosidase activity assay. GCase activity was measured using modifications of a previously published protocol (Mazzulli et al. 2011). Brain homogenates were further diluted with 1.11% bovine serum albumin, 0.28% Triton X-100, 0.28% taurocholic acid and 1.11 mM EDTA, pH 8 (all Sigma). Homogenates were then further diluted with buffer containing the fluorogenic substrate 4-MUGluc (1.11 mM, Sigma) in the presence or absence of 0.2 mM conduritol b epoxide (Sigma), a selective inhibitor of GCase. After a 1 h at 37°C, stop buffer was added and 4-MU fluorescence was quantified as above for α-Gal A. Selective GCase activity was determined by subtracting activity in the presence of GCase inhibitor from total activity and was expressed as nmol 4-MU substrate/mg protein in sample/h.

Cathepsin activity assays. Cat B and Cat D activities were assessed using assay kits from Sigma (Cat D) or Abnova (Cat B) as previously reported (Crabtree et al. 2013). These assays also utilize fluorogenic substrates that fluoresce upon reaction with endogenous Cat B or Cat D. Thirty µL of each brain homogenate combined with reaction buffer specific for each assay kit. After addition of fluorogenic substrates specific to each enzyme, samples were incubated for 2 h at 37°C followed by measurement of fluorescence. Assays were performed with or without pepstatin A or E64 (Sigma), selective inhibitors of Cat D or Cat B respectively. Following subtraction of residual fluorescence following treatment with Cat B or Cat D inhibitors, activity for each sample was normalized with respect to protein concentration.

Analysis of Gb_3 isoforms/analogs. PD and control brain tissue samples were homogenized using a bead mill to reach a concentration of 0.1 g/mL (methanol) as previously described (Boutin et al. 2016). The sample homogenates (100 µL) were spiked with 30 µL of Gb_3(d18:1)(C18:0)D_3 (0.04 µg/20 µL; Matreya, Pleasant Gap, PA) as the internal standard, saponified with KOH (1 M in methanol) and extracted with chloroform as described earlier (Auray-Blais and Boutin 2012; Manwaring et al. 2013). Samples were next re-suspended in 100 µL of methanol/5 mM ammonium formate/0.1% formic acid, separated by ultra-performance liquid chromatography (UPLC) (Acquity I-Class, Waters Corp., Milford, MA) and analyzed by tandem mass spectrometry (MS/MS) (Xevo TQ-S, Waters). The UPLC parameters are summarized in **Table 2**. The MS/MS analysis was performed in positive electrospray ionization using the multiple reaction monitoring (MRM) mode. The capillary and source offset voltages were 3200 and 60 V respectively. The source and desolvation temperatures were 250°C and 400°C, respectively. The desolvation and cone gas flows were respectively 550 and 150 L/h. A dwell time of 0.01 s, cone voltage of 30 V, collision energy of 25 V, and span of 0.2 Da were used for all molecules analyzed. **Supplemental Table 1** shows the MRM transitions for the 29 Gb_3 isoforms/analogs analyzed, the internal standard (Gb_3(d18:1)(C18:0)]D_3) and the C16:0 sphingomyelin (SM) analyzed for normalization. For Gb_3 isoforms/analogs, and for the internal standard, the fragments analyzed corresponded to the dehydrated ceramides. In the case of SM, the phosphocholine fragment was analyzed. For this molecule, we recorded the first natural isotope (1 x ^{13}C) for the molecular ion the fragment ion to decrease its signal and prevent detector saturation. For the calibration curve, a standard mixture of Gb_3 isoforms/analogs (Matreya) was spiked in a pooled control brain homogenate (100 µL). **Supplemental Table 2** shows the concentration of total Gb_3 and the seven most abundant Gb_3 isoforms/analogs in the different points of the calibration curve and in the quality control (QC) used for the method validation. The weight percentage of each Gb_3 isoform and analog in the standard mixture was evaluated assuming similar response factors for these molecules. The QC was used to measure the intra- and interday precision and accuracy (n = 5) for the seven spiked Gb_3 isoforms/analogs covering concentrations from 0.160 to 3.150 µg/g brain tissue. The QC was also used to evaluate the sample stability for 5 h at 22°C, 24 h at 4°C, 14 months at -20°C, and after two freeze/thaw cycles (n = 2). The stability of the prepared samples was also evaluated after 12 h in the auto sampler at 22^{o}C (n = 2). The recovery was evaluated by spiking the standard solution before and after the liquid-liquid extraction (n = 3). The limits of detection and of quantification for the seven spiked Gb_3 isoforms and analogs were defined as three and ten times the standard deviation of the concentrations measured for the intraday (n = 5).

Mass spectrometry analysis of lyso-Gb_3 isoforms/analogs in PD brain tissue samples. Lyso-Gb_3 and its analogs were analyzed in brain homogenates (100 µL; 0.1 g/mL MeOH) according to protocols previously published for the analysis of these molecules in plasma (Boutin et al. 2016, 2014). Brain tissue samples from α-Gal A -deficient and wild type control mice were also analyzed as positive and negative controls. The method validation was similar to the one performed for the Gb_3 isoforms/analogs, except that the QC was prepared by spiking standard lyso-Gb_3 (Matreya) in a pool of brain homogenate from healthy controls to reach a concentration of 40.0 pmol/g brain tissue.

Statistics. Analyses of clinical data and biochemical data were performed using Graph Pad Prism software and SAS software. Analyses of mass spectrometry data (levels of every Gb_3 isoform/analog and of total Gb_3) were statistically compared using PASW Statistics 18 software (SPSS, Quarry Bay, Hong Kong). Analysis of gender distribution in our cohort groups was tested for significance using the Pearson chi square test. Data were analyzed for normal distribution between groups using the Shapiro-Wilk test. If normal distributions ($p<0.05$) were not observed, these datasets were subjected to non-parametric analyses using either the Kruskal-Wallis or Mann-Whitney U test, with post analyses via Dunn's Multiple Comparison test. Normally distributed data sets were subjected to one-factor ANOVA. Significant ANOVAs were followed by post hoc analysis with the Bonferroni's Multiple Comparison test. Correlations between different endpoints were assessed using the non-parametric Spearman's test and stepwise multiple linear regressions. For all statistical analyses, a level of $p < 0.05$ was considered significant.

RESULTS

Analysis of clinical data

Clinical data are presented in **Table 1**. Analyses of clinical data from cases were performed two ways: 1) with Stage IIa PD and ILBD cases analyzed separately or 2) as combined. Significant differences were not observed for sex distribution or postmortem interval regardless of whether Stage IIa or ILBD cases were analyzed separately or as combined. A significant difference of age at death was observed when Stage IIa and ILBD cases were analyzed separately (1 way ANOVA, $p = 0.0186$) or as combined (1 way ANOVA, $p = 0.0037$). In both analyses, post hoc analysis revealed significant differences between Stage IV cases and either Stage IIa (*p=0.0177) or combined Stage IIa/ILBD cases (**p=0.0125). Disease duration was not significantly different with respect to cases with PD.

p129S-α-syn is increased in late-stage PD temporal cortex

Our first goal was to confirm an increased detection of p129S-α-syn immunoreactivity in late-stage PD temporal cortex **(Fig. 1)**. We quantified two prominent species of p129S-α-syn in homogenates from temporal cortex **(Fig. 1a)**, a ~17 kilodalton (kDa) species and high molecular weight species (> 75 kDa), as previously reported (Walker et al. 2013). Analysis of the 17 kDa species of p129S-α-syn revealed that Stage 0 control; $p = 0.0029$), Stage IIa PD/ILBD ($p = 0.0001$) and Stage III PD ($p = 0.0041$) groups lacked normal distribution. Subsequent non-parametric analysis revealed a significant difference ($p = 0.0025$) between groups for the 17 kDa species of p129S-α-syn, with post hoc analysis indicating significantly increased immunoreactivity in Stage IV PD (late-stage) compared to Stage IIa PD/ILBD but not to Stage III PD or Stage 0 control **(Fig. 1b)**. Analysis of high molecular weight species of p129S-α-syn (>75 kDa) revealed normally distributed data for all groups ($p > 0.05$), and a significant ANOVA ($p = 0.0104$). Subsequent post hoc analysis revealed significantly increased immunoreactivity for high molecular weight species of p129S-α-syn in Stage IV PD (late-stage) compared to Stage 0 control but not compared to Stage III PD or Stage IIa PD/ILBD **(Fig. 1b)**.

We also assessed levels of total α-syn 17 kDa monomer **(Fig. 1c)** in citrate-phosphate buffer homogenates from temporal cortex. One group (Stage IIa PD/ILBD) exhibited data lacking normal distribution ($p = 0.0045$). Subsequent non-parametric analysis revealed a lack of significance ($p = 0.5556$) between all groups **(Fig. 1d)**.

Alpha-Gal A levels and activity are decreased in late-stage PD temporal cortex in correlation with changes in α-syn species

We next assessed α-Gal A enzymatic activity in citrate-phosphate buffer homogenates from temporal cortex specimens with respect to Lewy body staging **(Fig. 2)**. Statistical analysis revealed normally distributed data for all groups ($p > 0.05$) and a significant ANOVA ($p = 0.0056$). Subsequent post hoc analysis indicated significantly decreased α-Gal A enzymatic activity in Stage IV PD (late-stage) compared to all other stages **(Fig. 2a)**. A significant negative correlation was also observed between decreasing α-Gal A activity and increasing 17 kDa p129S-α-syn and (Spearman's rho = -0.6154, $p < 0.0001$); **(Fig. 2b, Supplemental Table 3)**, but a significant correlation was not observed between α-Gal A activity and p129S-α-syn high MW species (Spearman's rho = -0.0.1011, $p = 0.494$); **(Fig. 2c, Supplemental Table 3)**. In addition, a significant positive correlation was observed between total α-syn monomer and α-Gal A activity (Spearman's rho = 0.5801, $p < 0.0001$); **(Fig. 2d, Supplemental Table 3)**.

Western blot analysis of α-Gal A was performed in temporal cortex homogenates in parallel to that of α-Gal A activity assay **(Fig. 3)**. Two bands were identified that were considered to be selective for α-Gal A: a 51 kDa "inactive" species and a 46 kDa "active" species **(Fig. 3a)**, as previously reported (Lemansky et al. 1987). Analysis of the 46 kDa "active" species of α-Gal A revealed normally distributed data for each group ($p > 0.05$), and a significant ANOVA ($p = 0.003$). Subsequent post hoc analysis revealed a significant decrease in the 46 kDa "active" species of α-Gal A in Stage IV PD (late-stage) compared to Stage 0 control and Stage IIa PD/ILBD, but not compared to Stage III PD **(Fig. 3b)**. The magnitude of decrease in the active species of α-Gal A observed by western blot analysis was similar to that observed for α-Gal A activity **(Figs. 2a, 3b)**. A significant positive correlation was observed between α-Gal A levels and activity (Spearman's rho = 0.3926, $p = 0.0058$); **(Fig. 3c**), further emphasizing the consistency of results obtained via these two different assays. However, unlike correlation analysis for α-Gal A activity, significant correlations were not observed between the 46 kDa species of α-Gal A and any species of α-syn measured in this study **(Supplemental Table 3)**.

Analysis of GCase activity

Because α-Gal A is in the same metabolism pathway as GCase, and because GCase deficiency was previously reported in postmortem PD brain (Gegg et al. 2012; Mazzulli et al. 2011; Murphy et al. 2014) we assayed for GCase activity in citrate-phosphate buffer homogenates from temporal cortex **(Fig. 4)**. Data were found to be normally distributed within groups ($p > 0.05$), but subsequent ANOVA indicated no significant difference in GCase activity with respect to Lewy body staging ($p = 0.2279$) **(Fig. 4a)**. However, a significant negative correlation was observed between decreasing GCase activity and increasing 17 kDa p129S-α-syn (Spearman's rho = -0.3802, $p = 0.0077$); **(Fig. 4b, Supplemental Table 3)**. Significant correlations were not observed between GCase activity and either high MW p129S-α-syn (Spearman's rho = -0.1258, $p = 0.3941$); **(Fig. 4c, Supplemental Table 3)** or total α-syn monomer (Spearman's rho = 0.1873, $p = 0.2025$); **(Fig. 4d, Supplemental Table 3)**. We also observed a significant positive correlation between GCase activity and α-Gal A activity (Spearman's rho = 0.4838, $p = 0.0005$) and α-Gal A 46 kDa "active" species (Spearman's rho = 0.2934, p = 0430); **(Supplemental Table 4)**, indicating that these two enzymes of the glycosphingolipid metabolism pathway are similarly affected in PD brain.

Since four PD cases were identified with *GBA1* mutations, we collated biochemical data separately from these cases to assess any tendencies for α-syn species, α-Gal A activity and protein levels and for GCase activity **(Supplemental Table 5)**. Relative GCase activity

appeared to follow the degree of mutation represented in each case. In the two cases identified as PD Stage III with heterozygous mutations in *GBA1*, average GCase activity was 70.97 ± 0.33% % of Stage 0 control, lower than the combined average of 99.12% for all 12 cases. GCase activity for one of the Stage IV PD cases identified with compound heterozygous mutations for *GBA1* was 25.6% of Stage 0 control, while activity for the Stage IV PD case with the homozygous mutation was 0%. The only noticeable trend observed for α-syn species in cases with *GBA1* mutations was lower p129S-α-syn monomer for stage III PD cases (0.05 ± 0.00), compared to 0.91 ± 1.17 for all stage III PD cases. Activity for α-Gal A appeared to trend higher for Stage IV PD cases with *GBA 1* mutations (98.82 ± 5.21%), compared to an average of 83.92 ± 19.58 % for all Stage IV PD cases. This trend for increased α-Gal A activity in the two Stage IV cases with *GBA1* mutations was paralleled by increased levels of α-Gal A 46 kDa/Actin (0.92 ± 0.22 compared to a combined average for all samples of 0.78 ± 0.21). Future investigation with increased sample size for cases with *GBA1* mutations would be needed to properly validate and interpret these trends.

Analysis of cathepsin activities

Previous studies have shown a strong correlation between the lysosomal aspartic acid protease Cat D and accumulation of α-syn (Chu et al. 2009; McGlinchey and Lee, 2015; Qiao et al. 2008; Sevlever et al. 2008) Thus we assayed for Cat D activity in homogenates from temporal cortex. Statistical analysis revealed a lack of normal distribution for data within two groups: Stage 0 control ($p = 0.0257$) and Stage III PD ($p = 0.0195$). Subsequent non-parametric analysis revealed a significant difference ($p = 0.014$), with post hoc analyses indicating a significant decrease in Cat D activity in Stage IV PD (late-stage) compared to Stage 0 control, but not compared to Stage III PD or Stage IIa PD/ILBD **(Fig. 5a)**. A significant negative correlation was observed between decreasing Cat D activity and increasing α-syn high MW species (Spearman's rho = -0.401, $p = 0.0047$) **(Supplemental Table 3)**. However, significant correlations were not observed between Cat D activity and either 17 kDa p129S-α-syn or total α-syn 17 kDa monomer **(Supplemental Table 3)**. Unlike that observed for GCase and α-Gal A, significant correlations were not observed for Cat D activity and either α-Gal A activity (Spearman's rho = 0.09369, $p = 0.5265$) or α-Gal A 46 kDa active species (Spearman's rho = 0.1106, $p = 0.4541$); **(Supplemental Table 4)**.

Recent evidence has also implicated a role for the cysteine protease Cat B in regulating the degradation and/or pathogenesis of α-syn (Freeman et al. 2013; McGlinchey and Lee, 2015; Tsujimura et al. 2015). Thus, we also assayed for Cat B activity in homogenates from temporal

cortex. Statistical analysis revealed a lack of normal distribution for data within three groups: Stage IIa/ILBD (p = 0.0045), Stage III PD (p = 0.0024) and Stage IV (p = 0.0241). Subsequent non-parametric analysis indicated a lack of significance between groups (p = 0.1997); (**Fig. 5b**). Similar to analysis of Cat D, a significant negative correlation was observed between decreasing Cat B activity and increasing α-syn high MW species (Spearman's rho = -0.401, p = 0.0047) **(Supplemental Table 3)**. However, significant correlations were not observed between Cat B activity and either 17 kDa p129S-α-syn or total α-syn 17 kDa monomer **(Supplemental Table 3)**. In addition, significant correlations were not observed for Cat B activity and either α-Gal A activity (Spearman's rho = 0.0695, p = 0.6425) or α-Gal A 46 kDa active species (Spearman's rho = 0.01729, p = 0.9802); **(Supplemental Table 4)**.

Analysis of LAMP-2 as a general lysosomal membrane marker

To determine the relationship between our analyses of lysosomal enzyme activity with an alternate lysosome marker, we assessed levels of lysosome-associated membrane protein-2 (LAMP-2) in citrate-phosphate buffer homogenates **(Fig. 5c-d)**. Western blot analysis indicated one LAMP-2 band migrating between 75-100 kDa **(Fig. 5c)**. Statistical analysis revealed a lack of normal distribution for one group, Stage IIa PD/ILBD (p = 0.0432). Subsequent non-parametric analysis revealed a significant difference (p = 0.0267), with post hoc analyses indicating a significant increase in LAMP-2 levels in Stage IV PD (late-stage) compared to Stage 0 control and Stage IIa PD/ILBD but not compared to Stage III PD **(Fig. 5d)**. Changes in LAMP-2 levels did not correlate with α-Gal A Activity, the 46 kDa "active" species of α-Gal A, GCase activity or Cat D activity **(Supplemental Table 3)**. However, we did observe a significant negative correlation between decreasing Cat B activity and increasing levels of LAMP-2 (Spearman's rho = -0.3474, p = 0.0225); **(Supplemental Table 3)**.

Analysis of Gb_3 isoforms/analogs

Table 3 shows a summary of the method validation results for the analysis of Gb_3 isoforms/analogs in human brain tissues. The intra- and interday precision and accuracy were ≤ 11.7% and ≤ 14.3% respectively. Samples were stable for at least 5 h at 22^{o}C, 24 h at 4^{o}C, 14 months at -20^{o}C, and after 2 freeze/thaw cycles (*n* = 2) with bias ≤ 16.5%. The prepared samples were also stable in the auto sampler at 22^{o}C for at least 12 h with bias ≤ 16.9%. The extraction recoveries ranged from 87.1 to 121.4% and the limits of detection from 0.003 to 0.024 µg/g brain tissue for the seven Gb_3 isoforms/analogs analyzed. The seven linear calibration curves presented mean correlation factors (R^2) ≥ 0 .988. For all 29 Gb_3 isoforms/analogs

analyzed, the calibration curve obtained with the standard with the closest molecular mass was used for quantification. **Supplemental Table 6** and **Fig. 6** show Gb_3 isoform/analog levels measured in different brain tissue samples, and **Supplemental Table 7** and **Fig. 7** the peak areas of Gb_3 isoforms/analogs normalized with the peak area of SM C16:0. One healthy control (ND_2) had very high levels of Gb_3 (C16:0) (6.4 µg/g brain tissue), Gb_3 (C18:0) (8.0 µg/g brain tissue) and Gb_3 (C18:1) (1.5 µg/g brain tissue) which significantly increased the mean values and the standard deviation for these Gb_3 isoforms in the control group. A verification of this sample was thus done by analyzing it twice from two different tissue homogenates. We obtained similar results for both analyses. According to the Shapiro-Wilk test applied to total Gb_3 isoform/analog, the ND and PDIII groups are not normally distributed ($p < 0.05$). For this reason, the Kruskall-Wallis non-parametric statistical test was chosen for the comparison of the four sample groups of this study. For the different Gb_3 isoforms/analogs, *p*-values ranged between 0.15 (Gb_3(C26:0)) and 0.97, not reaching the level of significance ($p < 0.05$) established *a priori*. Without taking into account the 4 PD individuals also having Gaucher disease (two in group III and two in group IV) the Kruskall-Wallis *p*-values ranged from 0.07 (Gb_3(C20:0)) to 0.94 and were still not statistically significant. After normalization of the results with SM C16:0 areas, the only significant difference observed when all the samples were taken in account with the Kruskall-Wallis test, was for Gb_3 (C16:1) ($p = 0.048$). The Mann-Whitney U test revealed that the most significant difference was between Stage III PD and Stage IV PD groups ($p = 0.012$). However, after application of the Bonferroni correction, the *p*-value increased to 0.072 and the difference between the two groups was not statistically significant. Finally, with SM normalization and after removing the four individuals with Gaucher disease, no significant difference was observed between the sample groups by the Kruskall-Wallis test (p-values ≥ 0.053). Data for Gb_3 isoforms and analogs was also collated specific to the four cases of Gaucher disease with *GBA1* mutations (**Supplemental Tables 8 and 9**). Several Gb_3 isoforms and analogs appeared to exhibit trends of increase or decrease specific to cases with *GBA1* mutations compared to the combined average for all cases in Stage III PD or Stage IV PD. Future studies are required with an increased sample size for cases with *GBA1* mutations, to confirm and properly interpret these observed trends Gb_3 isoforms and analogs and to determine their relevance to α-Gal A activity and α-syn species.

Lyso-Gb_3 and analog analysis. To verify if lyso-Gb_3 and its eight analogs might be detected in brain tissues with the protocol previously developed for plasma, we analyzed these molecules in brain specimens from homozygous Fabry mice. Fabry disease leads to

storage of lyso-Gb_3. Therefore, as expected, higher levels of lyso-Gb_3 and of some of its analogs were observed in brain tissue samples from Fabry mice compared to wild-type mice. These results are presented in **Supplemental Table 10**. **Supplemental Table 11** shows a summary of the results of the method validation for the analysis of lyso-Gb_3 in human brain tissues. Unfortunately, the lyso-Gb_3 limit of detection reached by this method (20.4 pmol/g brain tissue) was not sufficient to detect this molecule in PD brain samples (**Fig. 8**).

Correlation of Gb_3 analogs/isoforms to biochemical endpoints To determine any potential relationships between changes in Gb_3 analogs/isoforms with respect to α-Gal A activity or the 17 kDa species p129S-α-syn, correlation analyses were performed. **Table 4** indicates results of correlation analyses of Gb_3 analogs/isoforms normalized to brain weight, and **Table 5** indicates correlations with respect to Gb_3 analogs/isoforms normalized to brain SM. Several negative correlations were observed with both methods of normalization between different Gb_3 isoforms/analogs and either α-Gal A activity or levels of the 46 kDa "active" species of α-Gal A, such that increasing amounts Gb_3 analogs/isoforms correlated with decreasing α-Gal A activity/levels. In addition, several positive correlations were observed between different Gb_3 isoforms/analogs and the 17 kDa species p129S-α-syn, such that increasing amounts of Gb_3 analogs/isoforms correlate with increasing levels of p129S-α-syn. In comparison, significant negative correlations were observed between only two isoforms of Gb3 (C18:0, **Table 4**; C22:1Me, **Table 5**) and the 17 kDa species of p129S-α-syn, such that increases in p129S-α-syn correlated with decreases in these two Gb3 isoforms.

DISCUSSION

It is well established that function of the autophagy-lysosome pathway (ALP) is compromised in PD brain and may contribute to disease pathogenesis Anglade et al. 1997; Cook et al. 2012; Dehay et al. 2012, 2010; Mazzulli et al. 2011; Zhu et al. 2003). Examination of the ALP has led to the discovery of several candidate therapeutic targets and disease biomarkers. Several lysosome-associated proteins have been identified as altered in PD brain or in pre-clinical models of PD, in association with aberrant processing of α-syn (Cullen et al. 2001; Dehay et al. 2012, 2010; Gegg et al. 2012; Mangieri et al 2014; Mazzulli et al. 2011; Murphy et al. 2014; Qiao et al. 2008; Zhu et al. 2003). In addition, several studies indicate a strong correlation between altered lysosome function and α-syn-associated pathology and toxicity (Mazzulli et al. 2011; Qiao et al. 2008; Richter et al. 2014; Rocha et al. 2015; Sardi et al.

2013; Wustman et al. 2014). Results of our study indicate novel findings of α-Gal A deficiency in late-stage PD temporal cortex that also harbor the pathological accumulation of α-syn. Our demonstration of α-Gal A deficiency in postmortem PD brain corroborates findings of previous studies indicating α-Gal A deficiency in blood leukocytes of PD patients (Wu et al. 2008) and in blood samples of PD patients with mutations in *GBA1* that also exhibited increases in oligomeric α-syn (Pchelina et al. 2017). Levels of several Gb_3 isoforms also correlate positively with the pathological accumulation of p129S-α-syn and negatively with α-Gal A deficiency. Collectively our findings suggest the potential for α-Gal A and its glycosphingolipid metabolites to serve as putative candidate biomarkers and therapeutic targets for PD.

Both α-Gal A activity and levels of the 46 kDa "active" species of α-Gal A were approximately 20% lower in Stage IV PD temporal cortex. These values correlated significantly with each other, thus providing further corroboration of these results. The pathologic increase in p129S-α-syn also correlated with decreased α-Gal A activity, suggesting the potential for a cause-effect relationship between these events. However, the increase in p129S-α-syn did not correlate significantly with levels of the 46 kDa "active" species of α-Gal A, although the trend was negative as was observed between α-Gal A activity and p129S-α-syn. This may suggest that the pathological accumulation of p129S-α-syn may affect α-Gal A activity without significantly influencing α-Gal A processing to the active species. At this time, it is unknown if the pathological accumulation of α-syn negatively regulates α-Gal A activity, and/or if α-Gal A deficiency is responsible in part for the pathological accumulation of α-syn, hypotheses worthy of future investigation. Previous studies with GCase support the idea of a "pathological feedback loop" whereby GCase deficiency causes the accumulation of α-syn species, and/or excess α-syn causes a decrease in GCase activity (Mazzulli et al. 2011; Yap et al. 2013). Although we did not observe significant changes in GCase activity in PD brain as compared to previously published reports (Gegg et al. 2012; Mazzulli et al. 2011; Murphy et al. 2014), the significant negative correlation observed between decreasing activity with increasing p129S-α-syn supports their relative association. In addition, changes in GCase activity correlated significantly with those of α-Gal A activity and levels, suggesting their potential for cooperative involvement in PD. It will be important in the future to measure α-syn, α-Gal A and GCase simultaneously in brain regions such as the brain stem or substantia nigra, to determine if predicted loss of enzyme activity is more robust and occurs earlier with respect to the documented earlier pathological accumulation of α-syn in these brain regions (Beach et al. 2009).

Cat D is a lysosomal aspartic acid protease which has been shown previously to selectively degrade α-syn (Sevlever et al. 2008), and its deficiency has been shown in mice to

cause the aberrant accumulation of α-syn (Qiao et al. 2008). To our knowledge, this is the first report indicating a decrease in Cat D enzymatic activity in PD brain. Our findings corroborate the previous observation of decreased Cat D immunoreactivity in the substantia nigra of PD patients in association with the pathologic accumulation of α-syn (Chu et al. 2009). Despite recent reports indicating a role for Cat B in regulating the degradation and/or pathogenesis of α-syn (Freeman et al. 2013; McGlinchey and Lee, 2015; Tsujimura et al. 2015), we did not observe significant differences in Cat B activity in PD brain. However, for both Cat B and Cat D we observed a significant negative correlation between their decreasing activities with respect to increasing levels of high MW species of p129S-α-syn, suggesting that lysosomal proteases may have differential effects on the accumulation of α-syn species compared to those of lipid hydrolases (α-Gal A, GCase). This potential for diverging roles between cathepsins and α-Gal A is further supported by a lack of significant correlation between either Cat D or Cat B with α-Gal A activity or levels. It will be interesting to determine in the future if there is a causal relationship between cathepsin activity and of enzymes/lipids of the glycosphingolipid metabolism pathway, and their relative contributions to affecting the pathological accumulation of α-syn species in PD.

The significant increase in levels of LAMP-2 observed in late-stage PD temporal cortex suggests either an increase in lysosome number and/or size in late-stage PD brain, due possibly to a compromise in lysosome function (as suggested by results of α-Gal A and Cat D activity assays, and a significant negative correlation between LAMP-2 levels Cat B activity). This is in contrast to previously reported decreases in LAMP-2 or LAMP-2A (isoform selective for chaperone-mediated autophagy) in PD brain (Alvarez-Erviti et al. 2010; Murphy et al. 2014; Murphy et al. 2015). These discrepancies could be due to differences in how brain tissue was processed. We used a buffer lacking SDS, which is not compatible for α-Gal A and GCase activity assays, and assessed the “whole” fraction, whereas these other studies used either SDS-containing buffer and/or assessed a “lysosome-enriched” fraction. Future analysis of lysosome-enriched fractions from PD brain, and/or use of buffer systems similar to that of previously reported studies would more directly address these concerns. In addition, as glycosylation of LAMP proteins may affect the integrity and function of lysosomes (Cuervo and Dice 2000), it would be worthwhile in the future to carefully investigate the relative glycosylation state of LAMP-2 and other LAMP proteins with respect to other measures of lysosome function in PD brain.

While we did not observe significant changes in Gb_3 isoforms with respect to Lewy body staging of PD tissue, we did observe significant correlations between increases in several Gb_3 isoforms and either decreased α-Gal A activity, and/or increased p129S-α-syn. These findings

support further study of these Gb_3 isoforms for their potential as PD biomarkers or as contributors to α-syn pathogenesis. It is unclear at this time why a select number of Gb_3 isoforms exhibited significant negative correlations with respect to increasing levels of p129S-α-syn, or candidate mechanism(s) to explain their decrease in PD. Future studies incorporating a larger sample size of PD and control brain specimens would allow us to indicate the potential for identifying significant changes in specific isoforms with respect to Lewy body staging, as well as the potential to corroborate findings of the present study. In support of the argument that increasing levels of Gb_3 isoforms may contribute to PD pathogenesis, it has been suggested recently that increased glucosylceramide resulting from GCase deficiency can affect proper lysosomal function (Mazzulli et al. 2011; Gan-Or et al 2015). As α-Gal A and GCase are in the same glycosphingolipid metabolism pathway (Xu et al. 2010), an interconnectedness may exist between alterations of these two glycosphingolipid metabolism enzymes, the glycosphingolipids they metabolize and their putative interactions with the pathological accumulation of α-syn. These concepts are worthy of future study in the hopes of establishing novel biomarkers and therapeutics for PD.

ACKNOWLEDGMENTS

The research in this manuscript was supported by the following awards: Michael J Fox Foundation Access Data-Biospecimens Program (JJS and CAB); R21 NS093435-01 (JJS); NIGMS MERIT Postdoctoral Fellowship 5 K12 GM088010-05 (MPN); UAB AMC21 reload multi-investigator grant (JZ); NIHR01-NS064090 (JZ). We would also like to gratefully acknowledge Drs. Thomas Beach and Geidy Serrano at the Banner Sun Health Research Institute, and for Dr. Ken Valenzano of Amicus Therapeutics for providing assistance in establishing the α-Gal A activity assay in our laboratory. We also thank Dr. Gary Cutter (UAB Dept. Biostatistics) for statistical advice for data analysis. Finally, we wish to thank Waters Corp. for their technical and scientific support.

CONFLICTS OF INTEREST

Michael P. Nelson: None

Michel Boutin has received financial support for a salary from Shire and Sanofi-Genzyme and funds for traveling expenses from Waters Corp.

Tonia E. Tse: None

Hailin Lu: None

Emily D. Haley: None

Xiaosen Ouyang: None

Christiane Auray-Blais has received reimbursement for attending a symposium from Shire and Sanofi-Genzyme. She has received a fee for speaking or for organising education from Shire and Sanofi-Genzyme. She has also received research funds from Shire, Sanofi-Genzyme, BioMarin Pharmaceuticals and fees for consulting from Amicus Therapeutics. Finally, she has received funds from Waters Corp. for traveling expenses for lectures given.

John J. Shacka: None

REFERENCES

Alvarez-Erviti L, Rodriguez-Oroz MC, Cooper JM, Caballero C, Ferrer I, Obeso JA, Schapira AHV. Chaperone-mediated autophagy markers in Parkinson disease brains. *Arch Neurol*. 2010; 67: 1464-72.

Auray-Blais C, Boutin M. Novel Gb_3 Isoforms Detected in Urine of Fabry Disease Patients : A Metabolomic Study. *Curr. Med. Chem.*2012; 19: 3241-3252.

Anglade P, Vyas S, Javoy-Agid F, Herrero MT, Michel PP, Marquez J, Mouatt-Prigent A, Ruberg M, Hirsch EC, Agid Y. Apoptosis and autophagy in nigral neurons of patients with Parkinson's disease. *Histol. Histopathol.* 1997; 12: 25-31.

Beach TG, Sue LI, Walker DG, Roher AE, Lue L, Vedders L, Connor DJ, Sabbagh MN, Rogers J. The Sun Health Research Institute Brain Donation Program: description and experience, 1987-2007. Cell Tissue Bank. 2008; 9: 229-45.

Beach TG, Adler CH, Lue L, Sue LI, Bachalakuri J, Henry-Watson J, Sasse J, Boyer S, Shirohi S, Brooks R, Eschbacher J, White CL 3rd, Akiyama H, Caviness J, Shill HA, Connor DJ, Sabbagh MN, Walker DG, Arizona Parkinson's Disease Consortium. Unified staging system for Lewy body disorders: correlation with nigrostriatal degeneration, cognitive impairment and motor dysfunction. *Acta Neuropathologica*. 2009; 117: 613-634.

Benjamin ER, Flanagan JJ, Schilling A, Chang HH, Agarwal L, Katz E, Wu X, Pine C, Wustman B, Desnick RJ, Lockhart DJ, Valenzano KJ. The pharmacological chaperone 1-deoxygalactonojirimycin increases alpha-galactosidase A levels in Fabry patient cell lines. *J. Inherit. Metab. Dis.* 2009; 32: 424-440.

Beutler E, Kuhl W. Purification and properties of human alpha-galactosidases. J. Biol. Chem. 1972; 247: 195-200.

Borsini W, Giuliacci G, Torricelli F, Pelo E, Martinelli F, Scordo MR. Anderson-Fabry disease with cerebrovascular complications in two Italian families. *Neurol Sci*. 2002; 23: 49-53.

Boutin M, Lavoie P, Abaoui M, Auray-Blais C. Tandem Mass Spectrometry Quantitation of Lyso-Gb_3 and Six Related Analogs in Plasma for Fabry Disease Patients. *Curr. Protoc. Hum. Genet.* 90:17.23.1-17.23.9. doi: 10.1002/cphg.4

Boutin M, Sun Y, Shacka JJ, Auray-Blais C. Tandem Mass Spectrometry Multiplex Analysis of Glucosylceramide and Galactosylceramide Isoforms in Brain Tissues at Different Stages of Parkinson Disease. *Anal. Chem.* 2016; 88: 1856-1863.

Boutin M, Auray-Blais C. Multiplex Tandem Mass Spectrometry analysis of Novel Plasma Lys-Gb_3-Related analogues in Fabry Disease. *Anal. Chem*. 2014; 86: 3476-3483.

Braak H, Del TK, Rub U, de Vos RA, Jansen Steur EN Braak E. Staging of brain pathology related to sporadic Parkinson's disease. *Neurobiol. Aging.* 2003; 24: 197-211.

Brady RO. Enzymatic abnormalities in diseases of sphingolipid metabolism. *Clin. Chem.* 1967; 13: 565-577.

Buechner S, De Cristofaro MT, Ramat S Borsini W. Parkinsonism and Anderson Fabry's disease: a case report. *Mov. Disord.* 2006; 21: 103-107.

Chu Y, Dodiya H, Aebischer P, Olanow CW, Kordower JH. Alterations in lysosomal and proteasomal markers in Parkinson's disease: relationship to alpha-synuclein inclusions. *Neurobiol Dis*. 2009; 35: 385-398.

Conway KA, Lee SJ, Rochet JC, Ding TT, Williamson RE Lansbury PT, Jr. Acceleration of oligomerization, not fibrillization, is a shared property of both alpha-synuclein mutations linked to early-onset Parkinson's disease: implications for pathogenesis and therapy. *Proc. Natl. Acad. Sci. USA.* 2000; 97: 571-576.

Cook C, Stetler C, Petrucelli L Disruption of protein quality control in Parkinson's disease. *Cold Spring Harb. Perspect. Med*. 2012; 5: a0094323.

Crabtree D, Dodson M, Ouyang X, Boyer-Guittaut M, Liang Q, Ballestas ME, Fineberg N, Zhang J. Over-expression of an inactive mutant cathepsin D increases endogenous alpha-synuclein and cathepsin B activity in SH-SY5Y cells. *J. Neurochem*. 2013; 128: 950-961.

Cuervo AM, Dice JF. Regulation of lamp2 levels in the lysosomal membrane. *Traffic*. 2000; 1: 570-583.

Cullen V, Sardi SP, Ng J, Xu YH, Sun Y, Tomlinson JJ, Kolodziej P, Kahn I, Saftig P, Woulfe J, Rochet JC, Glicksman MA, Cheng SH, Grabowski GA, Shihabuddin LS, Schlossmacher MG. Acid β-glucosidase mutants linked to Gaucher disease, Parkinson disease and Lewy body dementia after α-synuclein processing. *Ann. Neurol*. 2011; 69: 940-953.

Danzer KM, Haasen D, Karow AR, Moussaud S, Habeck M, Giese A, Kretzschmar H, Hengerer B, Kostka M. Different species of alpha-synuclein oligomers induce calcium influx and seeding. *J. Neurosci.* 2007; 27: 9220-9232.

Danzer KM, Kranich LR, Ruf WP, Cagsal-Getkin O, Winslow AR, Zhu L, Vanderburg CR, McLean PJ. Exosomal cell-to-cell transmission of alpha synuclein oligomers. *Mol. Neurodegener.* 2012; 7: 42.

Dehay B, Ramirez A, Martinez-Vicente M, Perier C, Canron MH, Doudnikoff E, Vital A, Vila M, Klein C, Bezard E. Loss of P-type ATPase ATP13A2/PARK9 function induces general lysosomal deficiency and leads to Parkinson disease neurodegeneration. *Proc. Natl. Acad. Sci. USA.* 2012; 109: 9611-9616.

Dehay B, Bove J, Rodriguez-Muela N, Perier C, Recasens A, Boya P, Vila M. Pathogenic lysosomal depletion in Parkinson's disease. *J. Neurosci.* 2010; 30: 12535-12544.

Desplats P, Lee HJ, Bae EJ, Patrick C, Rockenstein E, Crews L, Spencer B, Masliah E, Lee SJ. Inclusion formation and neuronal cell death through neuron-to-neuron transmission of alpha-synuclein. *Proc. Natl. Acad. Sci. USA* 2009; 106: 13010-13015.

de Veber GA, Schwarting GA, Kolodny EH, Kowall NW. Fabry disease: immunocytochemical characterization of neuronal involvement. *Ann Neurol*. 1992; 31: 409-415.

Freeman D, Cedillos R, Choyke S, Lukic Z, McGuire K, Marvin S, Burrage AM, Sudholt S, Rana A, O'Connor C, Wiethoff CM, Campbell EM. Alpha-synuclein induces lysosomal rupture and cathepsin dependent reactive oxygen species following endocytosis. *PLoS One*. 2013; 25: e62143.

Gan-Or Z, Dion PA, Rouleau GA. Genetic perspective on the role of the autophagy-lysosome pathway in Parkinson disease. *Autophagy*. 2015; 11: 1143-57.

Gegg ME, Burke D, Heales SJ, Cooper JM, Hardy J, Wood NW Schapira AH. Glucocerebrosidase deficiency in substantia nigra of Parkinson disease brains. *Ann. Neurol*. 2012; 72: 455-463.

Gegg ME, Sweet L, Wang BH, Shihabuddin LS, Sardi SP, Schapira AH. No evidence for substrate accumulation in Parkinson brains with GBA mutations. *Mov. Disord*. 2015; 30: 1085-89.

Kaye EM, Kolodny EH, Logigian EL, Ullman MD. Nervous system involvement in Fabry's disease: clinicopathological and biochemical correlation. *Ann. Neurol*. 1988; 23: 505-509.

Khanna R, Soska R, Lun Y, Feng J, Frascella M, Young B, Brignol N, Pellegrino L, Sitaraman SA, Desnick RJ, Benjamin ER, Lockhart DJ Valenzano KJ. The pharmacological chaperone 1-deoxygalactonojirimycin reduces tissue globotriaosylceramide levels in a mouse model of Fabry disease. *Mol. Ther.* 2010; 18: 23-33.

Klucken J, Poehler AM, Ebrahimi-Fakhari D, Schneider J, Nuber S, Rockenstein E, Schlotzer-Schrehardt U, Hyman BT McLean PJ, Masliah E, Winkler J. Alpha-synuclein aggregation involves a bafilomycin A1-sensitive autophagy pathway. *Autophagy.* 2012; 8: 754-766.

Lee HJ, Cho ED, Lee KW, Kim JH, Cho SG, Lee SJ. Autophagic failure promotes the exocytosis and intercellular transfer of alpha-synuclein. *Exp. Mol. Med.* 2013; 45: e22.

Lee HJ, Khoshaghideh F, Patel S, Lee SJ. Clearance of alpha-synuclein oligomeric intermediates via the lysosomal degradation pathway. *J. Neurosci.* 2004; 24: 1888-1896.

Lemansky P, Bishop DF, Desnick RJ, Hasilik A von Figura K. Synthesis and processing of a-Galactosidase A in human fibroblasts. *J. Biol. Chem.* 1987; 262: 2062-2065.

Luk KC, Kehm V, Carroll J, Zhang B, O'Brien P, Trojanowski JQ, Lee VM. Pathological alpha-synuclein transmission initiates Parkinson-like neurodegeneration in nontransgenic mice. *Science.* 2012; 338: 949-953.

Luk KC, Song C, O'Brien P, Stieber A, Branch JR, Brunden KR, Trojanowski JQ Lee VM. Exogenous alpha-synuclein fibrils seed the formation of Lewy body-like intracellular inclusions in cultured cells. *Proc. Natl. Acad. Sci. USA.* 2009; 106: 20051-20056.

Lwin A, Orvisky E, Goker-Alpan O, LaMarca ME Sidransky E. Glucocerebrosidase mutations in subjects with parkinsonism. *Mol. Genet. Metab.* 2004; 81: 70-73.

Mader BJ, Pivtoraiko VN, Flippo HM, Klocke BJ, Roth KA, Mangieri LR, Shacka JJ. Rotenone inhibits autophagic flux prior to inducing cell death. *ACS Chem. Neurosci.* 2012; 3: 1063-1072.

Mangieri LR, Mader BJ, Thomas CE, Taylor CA, Luker AM, Tse TE, Huisingh C and Shacka JJ. ATP6V0C knockdown in neuroblastoma cells alters autophagy-lysosome pathway function and metabolism of proteins that accumulate in neurodegenerative disease. *PLOS One*. 2014; 9: e93257.

Manwaring V, Boutin M, Auray-Blais C. A Metabolomic Study To Identify New Globotriaosylceramide-Related Biomarkers in the Plasma of Fabry Disease Patients. *Anal. Chem.* 2013; 85: 9039-9048.

Mazzulli, JR, Xu, YH, Knight, AL, McLean, PJ, Caldwell, GA, Sidransky, E, Grabowski, GA Krainc D 2011. Gaucher disease glucocerebrosidase and alpha-synuclein form a bidirectional loop in synucleinopathies. *Cell*. 2011; 146: 37-52.

McGlinchey RP, Lee JC. Cysteine cathepsins are essential in lysosomal degradation of α-synuclein. *Proc. Natl. Acad. Sci. USA*. 2015; 112: 9322-9327.

Murphy KE, Gysbers A, Abbott SK Spiro AS, Furuta A, Cooper A, Garner B, Kabuta T, Halliday GM. Lysosomal-associated membrane protein 2 isoforms are differentially affected in early Parkinson's disease. *Mov. Disord*. 2015; 30: 1639-1647.

Murphy KE, Gysbers A, Abbott SK, Tayebi M, Kim WS, Sidransky E, Cooper A, Garner B Halliday GM. Reduced glucocerebrosidase is associated with increased alpha-synuclein in sporadic Parkinson's disease. *Brain.* 2014; 137: 834-848.

Nelson MP, Tse TE, DB OQ, Percival SM, Jaimes EA, Warnock DG, Shacka JJ. Autophagy-lysosome pathway associated neuropathology and axonal degeneration in the brains of alpha-galactosidase A-deficient mice. *Acta Neuropathol. Commun.* 2014; 2:20.

Pchelina S, Emelyanov A, Baydakova G, Andoskin P, Senkevich K, Nikolaev M, Miliukhina I, Yakimovskii A, Timofeeva A, Fedotova E, Abramycheva N, Usenko T, Kulabukhova D, Lavrinova A, Kopytova A, Garaeva L, Nuzhnyi E, Illarioshkin S, Zakharova E. Oligomeric α-synuclein and glucocerebrosidase activity levels in GBA-associated Parkinson's disease. *Neurosci. Lett*. 2017; 636: 70-76.

Pivtoraiko VN, Harrington AJ, Mader BJ, Luker AM, Caldwell GA, Caldwell KA, Roth KA, Shacka JJ. Low-dose bafilomycin attenuates neuronal cell death associated with autophagy-lysosome pathway dysfunction. *J. Neurochem.* 2010; 114: 1193-1204.

Polymeropoulos MH, Lavedan C, Leroy E, Ide SE, Dehejia A, Dutra A, Pike B, Root H, Rubenstein J, Boyer R, Stenroos ES, Chandrasekharappa S, Athanassiadou A, Papapetropoulos T, Johnson WG, Lazzarini AM, Duvoisin RC, Di Iorio G, Golbe LI Nussbaum RL. Mutation in the alpha-synuclein gene identified in families with Parkinson's disease. *Science*. 1997; 276: 2045-2047.

Qiao L, Hamamichi S, Caldwell KA, Caldwell GA, Yacoubian TA, Wilson S, Xie ZL, Speake LD Parks R, Crabtree D, Liang Q, Crimmins S, Schneider L, Uchiyama Y, Iwatsubo T, Zhou Y, Peng L, Lu Y, Standaert DG, Walls KC, Shacka JJ, Roth KA, Zhang J. Lysosomal enzyme cathepsin D protects against alpha-synuclein aggregation and toxicity. *Mol.Brain.* 2008; 1: 1-18.

Richter F, Fleming SM, Watson M, Lemesre V, Pellegrino L, Ranes B, Zhu C, Mortazavi F, Mulligan CK, Sioshansi PC, Hean S, De La Rosa K, Khanna R, Flanagan J, Lockhart DJ,

Wustman BA, Clark SW, Chesselet MF. A GCase chaperone improves motor function in a mouse model of synucleinopathy. *Neurotherapeutics*. 2014; 11: 840-856.

Rocha EM, Smith GA, Park E, Cao H, Brown E, Hayes MA, Beagan J, McLean JR, Izen SC, Perez-Torres E, Hallett PJ, Isacson O. Glucocerebrosidase gene therapy prevents α-synucleinopathy of midbrain dopamine neurons. *Neurobiol Dis*. 2015; 82: 495-503.

Sardi SP, Clarke J, Viel C, Chan M, Tamsett TJ, Bu J, Sweet L, Passini MA, Dodge JC, Yu WH, Sidman RL, Cheng SH, Shihabuddin LS. Augmenting CNS glucocerebrosidase activity as a therapeutic strategy for parkinsonism and other Gaucher-related synucleinopathies. *Proc. Natl. Acad. Sci. USA.* 2013; 110: 3537-3542.

Sarkar S, Davies JE, Huang Z, Tunnacliffe A, Rubinsztein DC. Trehalose, a novel mTOR-independent autophagy enhancer, accelerates the clearance of mutant huntingtin and alpha-synuclein. *J. Biol. Chem.* 2007; 282: 5641-5652.

Sevlever D, Jiang P, Yen SH. Cathepsin D is the main lysosomal enzyme involved in the degradation of alpha-synuclein and generation of its carboxy-terminally truncated species. *Biochemistry*. 2008; 47: 9678-87.

Shacka JJ, Roth KA, Zhang J. The autophagy-lysosomal degradation pathway: role in neurodegenerative disease and therapy. *Front. Biosci*. 2008; 13: 718-736.

Song JX, Lu JH, Liu LF, Chen LL, Durairajan SS, Yue Z, Zhang HQ, Li M. HMGB1 is involved in autophagy inhibition caused by SNCA/α-synuclein overexpression: a process modulated by the natural autophagy inducer corynoxine B. *Autophagy*. 2014; 10: 144-154.

Singleton AB, Farrer M, Johnson J, Singleton A, Hague S, Kachergus J, Hulihan M, Peuralinna T, Dutra A, Nussbaum R, Lincoln S, Crawley A, Hanson M, Maraganore D, Adler C, Cookson MR, Muenter M, Baptista M, Miller D, Blancato J, Hardy J, Gwinn-Hardy K. Alpha-synuclein locus triplication causes Parkinson's disease. *Science*. 2003; 302: 841.

Spillantini MG, Schmidt ML, Lee VM, Trojanowski JQ, Jakes R Goedert M. Alpha-synuclein in Lewy bodies. *Nature.* 1997; 388: 839-840.

Sung J, Hayano M, Mastri A, Desnick R. Neuropathology and neural glycosphingolipid deposition in Fabry's disease*. Excerpta Med Cong Ser*. 1975; 1: 267.

Sybertz E Krainc D. Development of targeted therapies for Parkinson disease and related synucleinopathies. *J. Lipid Res*. 2014; 55: 1966-2003.

Tsujimura A, Taguchi K, Watanabe Y, Tatebe H, Tokuda T, Mizuno T, Tanaka M. Lysosomal enzyme cathepsin B enhances the aggregate forming activity of exogenous α-synuclein fibrils. *Neurobiol. Dis*. 2015; 73: 244-253.

Volpicelli-Daley LA, Luk KC, Patel TP, Tanik SA, Riddle DM, Stieber A, Meaney DF, Trojanowski JQ, Lee VM. Exogenous alpha-synuclein fibrils induce Lewy body pathology leading to synaptic dysfunction and neuron death. *Neuron.* 2011; 72: 57-71.

Walker DG, Lue LF, Adler CH, Shill HA, Caviness JN, Sabbagh MN, Akiyama H, Serrano GE, Sue LI, Beach TG; Arizona Parkinson Disease Consortium. Changes in properties of serine 129

phosphorylated alpha-synuclein with progression of Lewy-type histopathology in human brains. *Exp. Neurol.* 2013; 240: 190-204.

Winslow AR, Chen CW, Corrochano S, Acevedo-Arozena A, Gordon DE, Peden AA, Lichtenberg M, Menzies FM, Ravikumar B, Imarisio S, Brown S, O'Kane CJ, Rubinsztein DC. α-Synuclein impairs macroautophagy: implications for Parkinson's disease. *J. Cell Biol*. 2010; 190: 1023-1037.

Wu G, Yan B, Wang X, Feng X, Zhang A, Xu X, Dong H. Decreased activities of lysosomal acid alpha-D-galactosidase A in the leukocytes of sporadic Parkinson's disease. *J. Neurol. Sci*. 2008; 271: 168-173.

Wu G, Pang S, Feng X, Zhang A, Li J, Gu K, Huang J, Dong H, Yan B. Genetic analysis of lysosomal alpha-galactosidase A gene in sporadic Parkinson's disease. *Neurosci. Lett*. 2002; 23: 49-53.

Wustman BA, Clark SW, Chesselet MF. A GCase Chaperone Improves Motor Function in a Mouse Model of Synucleinopathy. *Neurotherapeutics.* 2014; 11: 840-856.

Xu Y-H, Barnes S, Sun Y Grabowski GA. Multi-system disorders of glycosphingolipid and ganglioside metabolism. *J. Lipid Re*s. 2010; 51: 1643-1675.

Yap TL, Velayati A, Sidransky E, Lee JC. Membrane-bound α-synuclein interacts with glucocerebrosidase and inhibits enzyme activity. *Mol. Genet. Metab*. 2013; 108: 56-64.

Zhu JH, Guo F, Shelburne J, Watkins S, Chu CT. Localization of phosphorylated ERK/MAP kinases to mitochondria and autophagosomes in Lewy body diseases. *Brain Pathol.* 2003; 13: 473-481.

FIGURE LEGENDS

Figure 1. Analysis of α-syn species in PD brain homogenates. (***a***) Representative western blot analysis for p129S-α-syn and total α-syn (***c***) from citrate-phosphate buffer homogenates of temporal cortex specimens staged with respect to α-syn-positive Lewy bodies (Beach et al 2009). Species of α-syn including ***(b)*** p129S-α-syn (17 kDa and high molecular weight species > 75 kDa) were normalized to Actin loading control (42 kDa) and expressed as mean ± SD relative to Stage 0 control (*n* = 12 cases/stage). Analysis of the 17 kDa species of p129S-α-syn: there were three groups with data lacking normal distribution: Stage 0 control ($p = 0.0029$), Stage IIa PD/ILBD ($p = 0.0001$) and Stage III PD ($p = 0.0041$). Subsequent non-parametric Kruskal-Wallis test indicated a significant difference ($p = 0.0025$) between groups. Dunn's post hoc test indicated a significant increase in Stage IV PD (late-stage) compared to Stage IIa PD/ILBD (*$p < 0.05$) but not to Stage III PD or Stage 0 control. Analysis of α-syn high-molecular weight species: Data were found to be normally distributed within groups ($p > 0.05$). Subsequent ANOVA indicated significance between groups ($p = 0.0104$); Bonferroni's post hoc test indicated a significant increase in Stage IV PD (late-stage) compared to Stage 0 control (CTL), **$p < 0.05$ but not compared to Stage III PD or Stage IIa PD/ILBD. (***c***) Representative western blot analysis for total α-syn; (***d***) the 17 kDa α-syn monomer was normalized to Actin loading control (42 kDa) and was expressed as mean ± SD relative to Stage 0 control (*n* = 12 cases/stage). Analysis of total α-syn 17 kDa monomer: One group (Stage IIa PD/ILBD) exhibited data lacking normal distribution ($p = 0.0045$). Subsequent non-parametric Kruskal-Wallis test revealed a lack of significance ($p = 0.5556$) between groups.

Figure 2. Alpha-Gal A activity is decreased in late-stage PD brain homogenates and correlates with changes in α-syn species. (***a***) Alpha-Gal A enzymatic activity from citrate-phosphate buffer homogenates of temporal cortex specimens staged with respect to α-syn-positive Lewy bodies was quantified as nmol 4-MU substrate/mg protein/ h and expressed as mean ± SD % of activity observed in Stage 0 control specimens, *n* = 12 cases/stage. Data within groups were found to be normally distributed ($p > 0.05$). Subsequent ANOVA indicated significance between groups ($p = 0.0056$); Bonferroni's post hoc test indicated a significant increase in Stage IV PD (late-stage) compared to all other stages (*$p < 0.05$). Correlation analyses revealed (***b***) a significant negative relationship between 17 kDa p129S-α-syn and decreasing α-Gal A activity (Spearman's rho = -0.6154, $p < 0.0001$), (***c***) a lack of significance between a-Gal A activity and α-syn high-molecular weight species (Spearman's rho = -0.1011, p

=0.494) and (***d***) a significant positive relationship between total α-syn monomer and α-Gal A activity (Spearman's rho = 0.5113, p = 0.0002).

Figure 3. Alpha-Gal A levels are decreased in late-stage PD brain homogenates in correlation with increased p129S-α-syn. (***a***) Representative western blot analysis for α-Gal A from citrate-phosphate buffer homogenates of temporal cortex specimens staged with respect to α-syn-positive Lewy bodies. Two bands were considered to be selective for α-Gal A: the 51 kDa "inactive" precursor and the 46 kDa "active" species (Lemansky et al 1987 PMID 3029062). (***b***) The 46 kDa "active" species was normalized to Actin loading control (42 kDa) and expressed as mean ± SD relative to Stage 0 control, *n* = 12 cases/stage. Statistical analysis indicated normally distributed data for each group ($p > 0.05$), and a significant ANOVA ($p = 0.003$). Bonferroni's post hoc test indicated a significant decrease in the 46 kDa "active" species of α-Gal A in Stage IV PD (late-stage) compared to Stage 0 control and Stage IIa PD/ILBD (*$p < 0.05$) but not compared to Stage III PD. Correlation analyses (***c***) indicated a significant positive relationship between α-Gal A 46 kDa "active" species and α-Gal A activity (Spearman's rho = 0.3926, p = 0.0058).

Figure 4. Analysis of GCase activity in PD brain homogenates. (***a***) GCase activity assay of citrate-phosphate buffer homogenates from temporal cortex (quantified as nmol 4-MU substrate/mg protein/ h and expressed as mean± SD, % activity observed in Stage 0 control, *n* = 12 cases/stage. Data were normally distributed data within each group ($p > 0.05$). Subsequent ANOVA revealed no significant differences with respect to Lewy body staging ($p > 0.05$). Correlation analyses indicated (***b***) a significant negative relationship between decreasing GCase activity and increasing levels of 17 kDa p129S-α-syn (Spearman's rho = -0.3802, p = 0.0077); and no significant correlations between GCase activity and (***c***) a significant positive relationship between GCase activity and either α-syn high-molecular weight species (Spearman's rho = -0.1258, p = 0.3941) or total α-syn monomer (Spearman's rho = 0.1873, p = 0.2025).

Figure 5. Analysis of additional lysosome markers. (***a***) Analysis of Cat D activity (normalized to mg protein/sample and expressed as mean± SD, % activity observed in Stage 0 control specimens, *n* = 12 cases/stage) revealed a lack of normal distribution for two groups: Stage 0 control (p = 0.0257) and Stage III PD (p = 0.0195). Subsequent non-parametric Kruskal-Wallis test revealed a significant difference (p = 0.014). Dunn's post hoc test indicated a significant decrease in Cat D activity in Stage IV PD (late-stage) compared to Stage 0 control (*p < 0.05) but not compared to Stage III PD or Stage IIa PD/ILBD. (***b***) Analysis of Cat B activity (normalized to mg protein/sample and expressed as mean± SD, % activity observed in Stage 0 control specimens, *n* = 11-12 cases/stage) revealed a lack of normal distribution for three groups: Stage IIa/ILBD (p = 0.0045), Stage III PD (p = 0.0024) and Stage IV (p = 0.0241). Subsequent non-parametric analysis via Kruskal-Wallis test revealed no significant differences between groups (p = 0.1997). (***c***) Representative western blot analysis for LAMP-2 from citrate-phosphate buffer homogenates of temporal cortex specimens staged with respect to α-syn-positive Lewy bodies. (***d***) The ~75 kDa LAMP-2 band was normalized to Actin loading control (42 kDa) and expressed as mean ± SD relative to Stage 0 control (*n* = 12 cases/stage). Statistical analysis revealed a lack of normal distribution for one group, Stage IIa PD/ILBD (p = 0.0432). Subsequent analysis via non-parametric Kruskal-Wallis test revealed a significant difference (p = 0.0267), with Dunn's post hoc test indicating a significant increase in LAMP-2 levels in Stage IV PD (late-stage) compared to Stage 0 control and Stage IIa PD/ILBD (*p < 0.05) but not compared to Stage III PD.

Figure 6. Levels of Gb_3 isoforms/analogs in brain tissue samples from Stage 0 control, Stage IIa PD/ILBD, Stage III PD and Stage IV PD, were determined by UPLC and MS-MS analysis and were normalized to brain tissue weight. Data are expressed as mean ± SD, *n* = 12 cases/stage.

Figure 7. Levels of Gb_3 isoforms/analogs were determined by UPLC and MS-MS analysis and normalized to SM C16:0 peak area, in brain tissue samples from Stage 0 control, Stage IIa PD/ILBD, Stage III PD and Stage IV PD. Data are expressed as mean ± SD, *n* = 12 cases/stage. The SM C16:0 peak area was measured using the first natural isotope (1 x ^{13}C).

Figure 8. Ion chromatograms of lyso-Gb_3 in: A) PD brain tissue pool; B) PD brain tissue pool spiked with lyso-Gb_3.

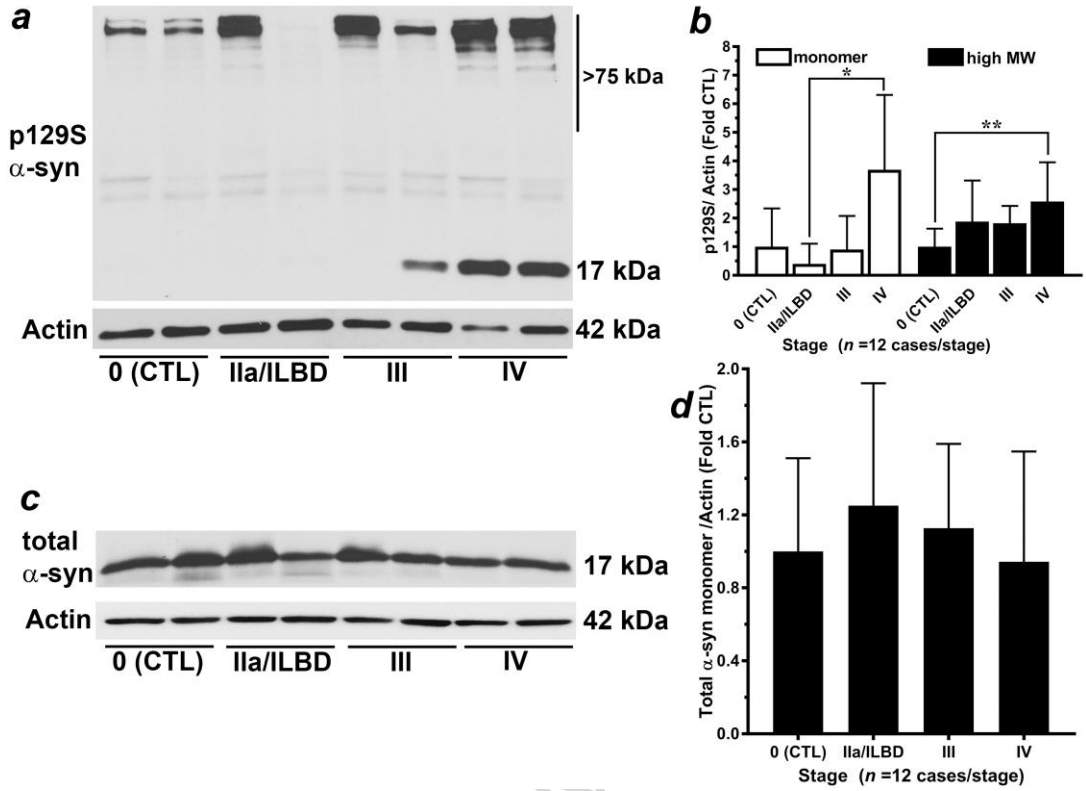

Fig. 1

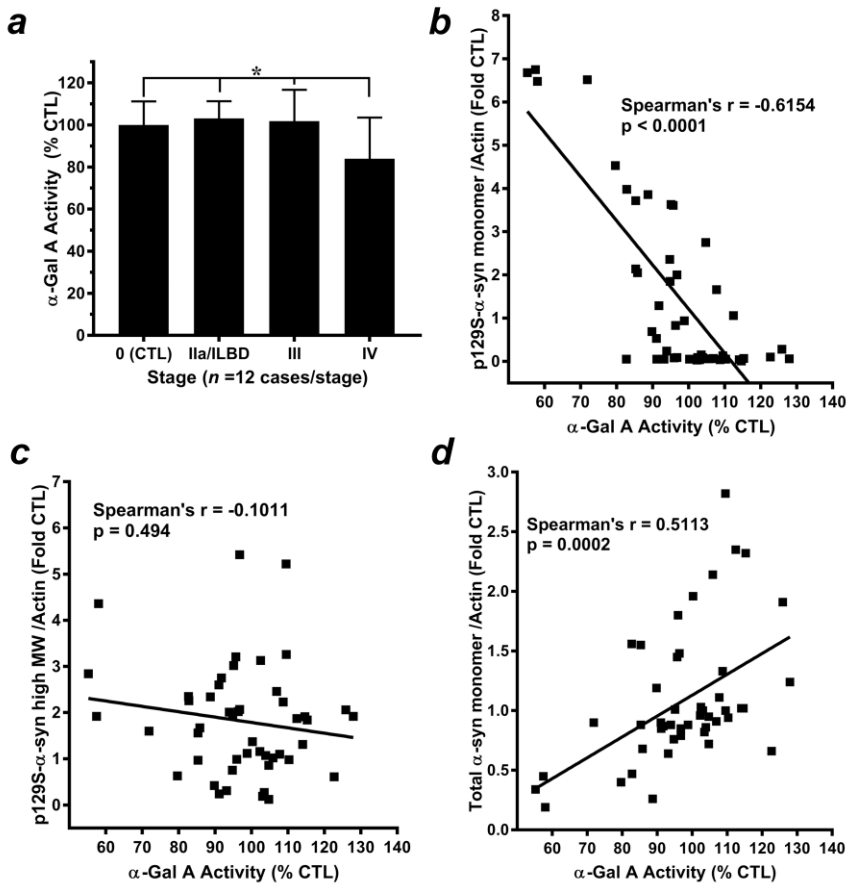

Fig. 2

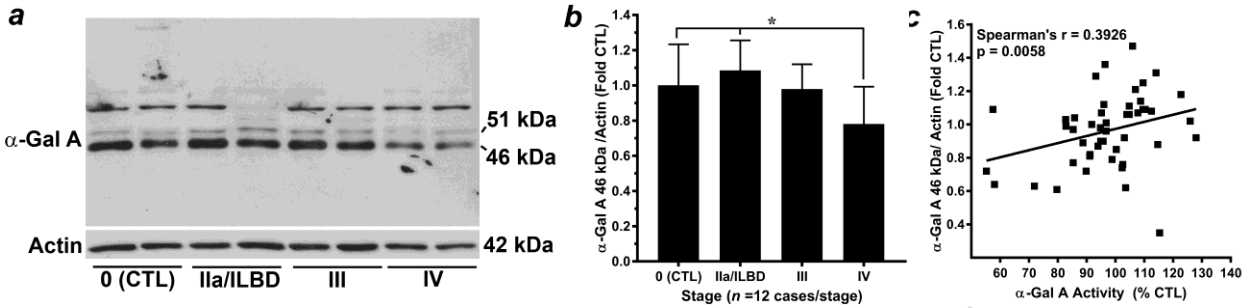

Fig. 3

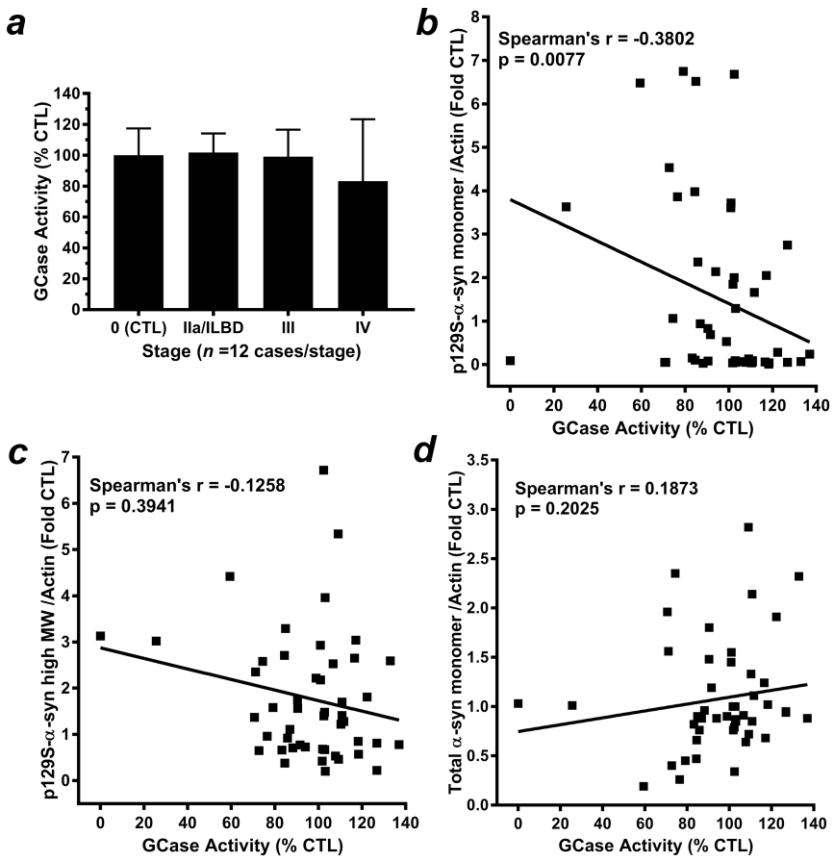

Fig. 4

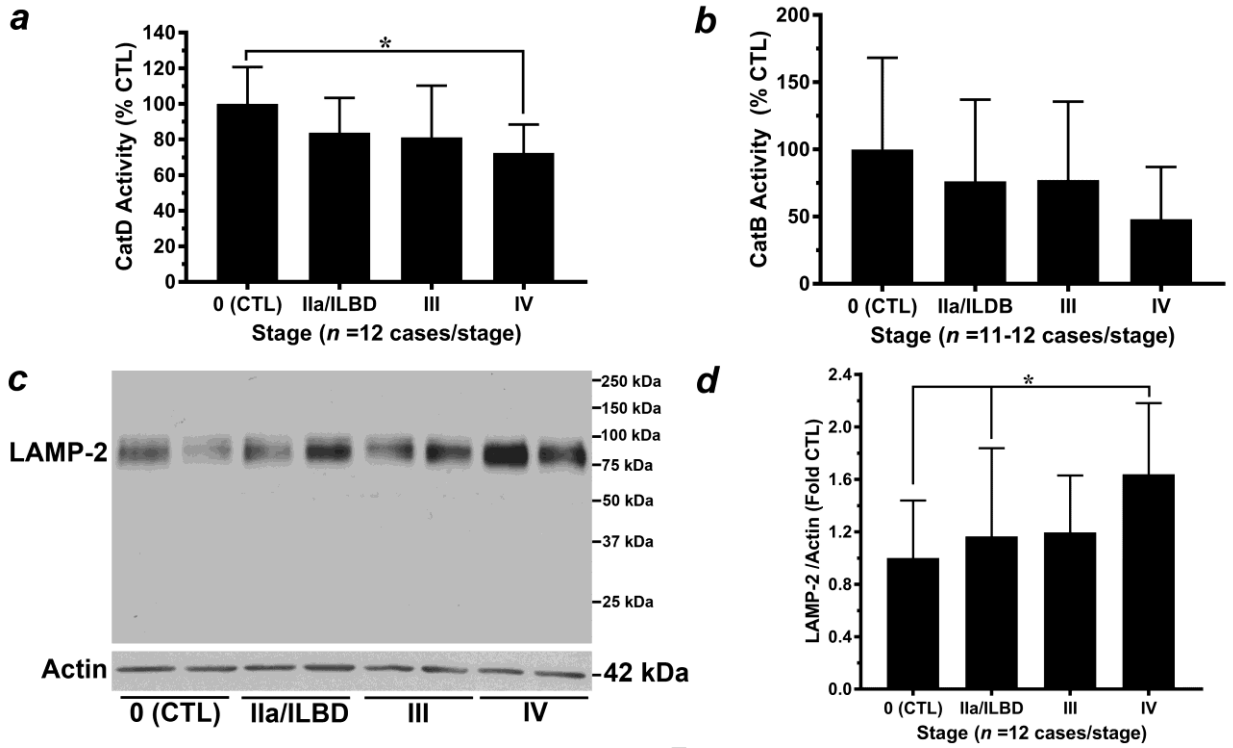

Fig. 5

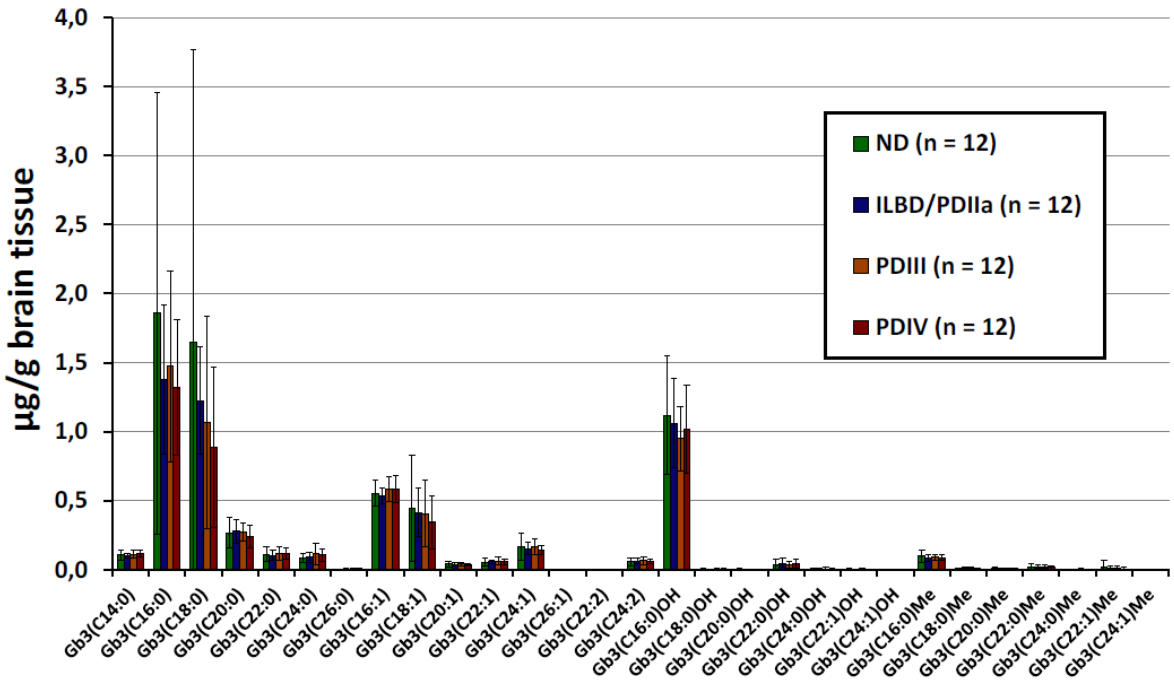

Fig. 6

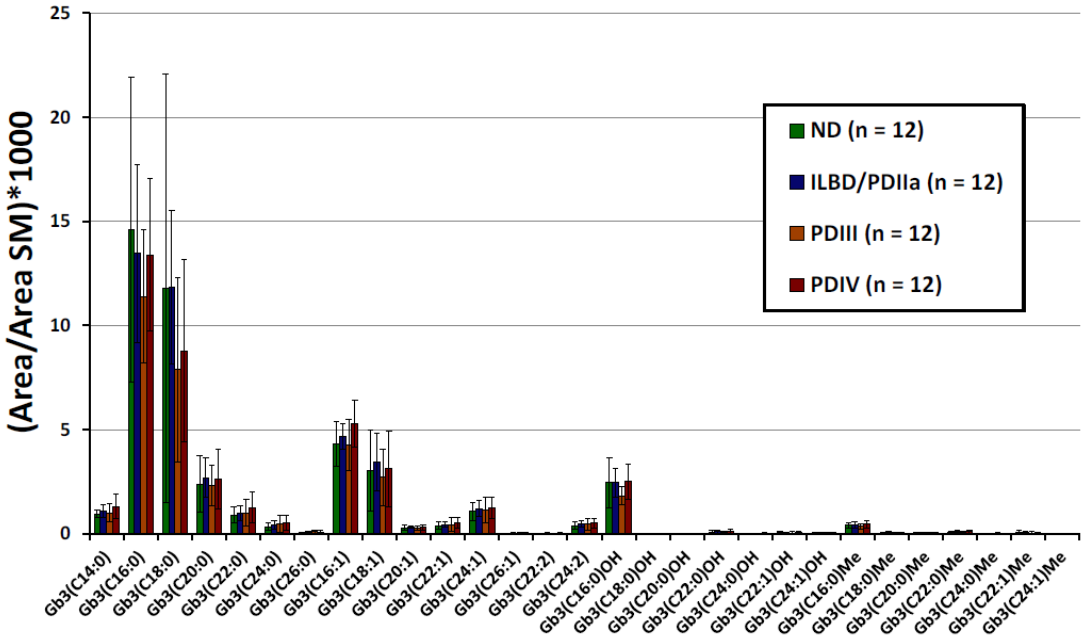

Fig. 7

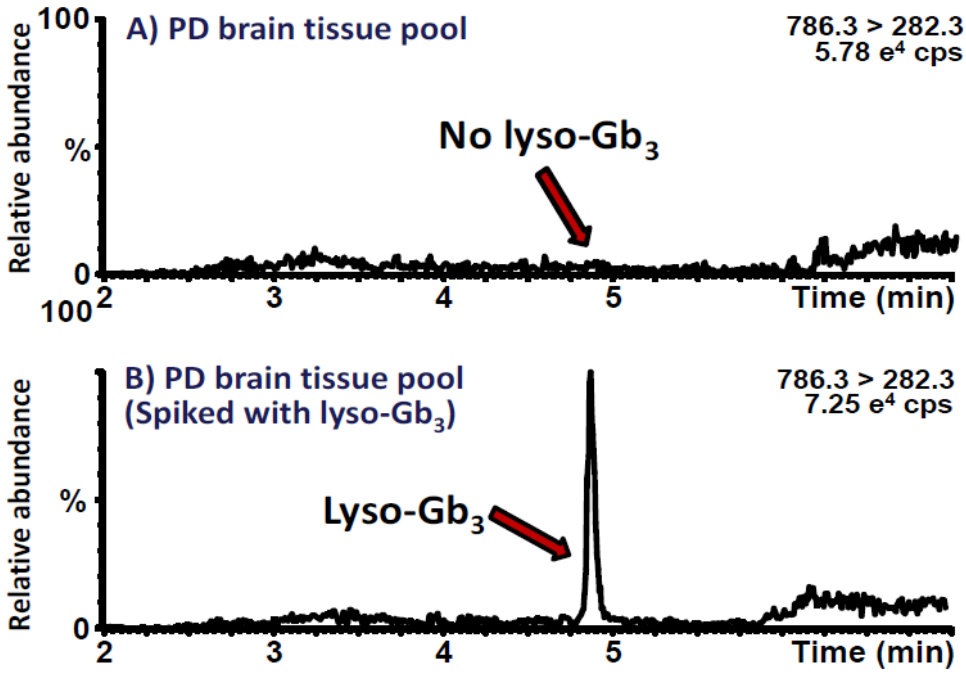

Fig. 8

Table 1. Summary of Clinical Data

Unified Lewy Body Stage[a]	***Stage 0 (Control)***	***Incidental Lewy Body Disease (ILDB)***[b]	***Stage IIa***[b]	***Stage III***	***Stage IV***	***Stage IIa plus ILDB***
Sex (M:F)[c]	10:2	5:1	4:2	9:3	8:4	9:3
Disease duration (years)[d]	N/A	N/A	10.83 ± 7.41	16.67 ±8.35	17.33 ±7.77	N/A
Age at death (years)[e]	80.58 ±9.38	84.67 ±4.13	89.00 ±2.37*	80.00 ±5.77	79.92 ±6.42	86.83 ±3.93**
Post-mortem interval (hr)[f]	2.85 ±0.53	2.65 ±0.54	3.05 ±0.65	3.20 ±0.63	2.85 ±0.59	2.85 ±0.60

[a]Synuclein/Lewy body stage, defined as previously described (Beach *et al* 2009).

[b]Due to a relative lack of availability of Stage IIa cases for our study, equal numbers of incidental Lewy body disease cases (with Lewy body pathology limited to olfactory bulb and brainstem) were combined with Stage IIa cases for experimental analyses (far right column).

[c]Differences between groups were not observed when Stage IIa and ILDB cases were analyzed separately (Chi-square, p=0.8557) or were combined (Chi-square, p=0.8281).

[d]Differences were not observed between Stage IIa, Stage III and Stage IV cases (1-way ANOVA, p=0.2484).

[e]Significant 1-way ANOVAs were observed when Stage IIa and ILDB cases were either analyzed separately (p=0.0186) or as combined (p=0.0137). In both cases, post hoc analysis revealed significant differences between Stage IV and either Stage IIa (*p=0.0177) or combined Stage IIa/ILDB cases (**p=0.0125).

[f]Differences between groups were not observed when Stage IIa and ILDB cases were analyzed separately (1-way ANOVA, p=0.3483) or were combined (1-way ANOVA, p=0.3755).

Table 2 UPLC method for the analysis of Gb_3 isoforms and analogs, and sphingomyelin (C16:0) in PD brain tissue samples.

Column	Acquity UPLC® BEH C8; Waters Corp. Lenght: 50 mm Internal diameter: 2.1 mm Particle diameter: 1.7 µM
Column temperature	22 °C
Weak wash solvent	50% methanol/0.1% formic acid/ 5 mM ammonium formate/water
Strong wash solvent	0.1% formic acid/methanol
Mobile phase A	0.1% formic acid/5 mM ammonium formate/ methanol
Mobile phase B	5% methanol/0.1% formic acid/ 5 mM ammonium formate/water
Gradient	0-1 min → 50%A 1-6 min → 50-80%A 6-12 min → 80-100%A 15-20 min → 50%A
Flow rate	0.5 mL/min
Injection volume	7.5 µL
Injection mode	Partial loop with needle overfill
Autosampler temperature	22 °C

Table 3. Summary of the method validation results for the analysis of Gb_3 isoforms and analogs in human brain tissue samples.

Gb_3 isoforms/analogs	C24:0	C22:0	(C24:0)OH	C24:1	(C24:1)OH	C26:0	C22:0Me
Spiked Conc (µg/g brain tissue)	3.150	1.248	1.050	0.480	0.425	0.263	0.160
Intraday (n = 5)							
Precision: RSD (%)	8.4	7.8	6.0	10.4	6.8	8.4	11.7
Accuracy: Bias (%)	-2.6	-3.0	-8.5	-3.4	-3.4	-0.9	5.6
Interday (n = 5)							
Precision: RSD (%)	2.1	3.9	3.3	6.5	11.9	2.0	3.8
Accuracy: Bias (%)	1.2	-0.3	-2.9	-3.4	-14.3	-4.5	-1.1
Stability (n = 2)							
(5 h, 22°C) Bias (%)	-8.2	-9.2	-12.8	-12.7	-7.2	-12.5	-16.2
(24 h, 4°C) Bias (%)	6.7	-4.4	16.5	4.2	1.6	7.0	2.3
(18 days, -20°C) Bias (%)	-4.8	-0.5	-5.1	-2.0	-2.5	-6.5	0.8
(14 months, -20°C) Bias (%)	5.3	-11.2	1.1	-15.9	7.2	4.4	0.0
(2 freeze/thaw cycles) Bias (%)	11.8	14.1	14.1	11.7	14.6	12.1	15.9
(12 h in injector, 22°C) Bias (%)	0.8	3.4	3.5	1.8	1.5	4.6	16.9
Recovery (%)	90.2	87.1	100.1	92.9	90.8	93.4	121.4
LOD (µg/g brain tissue)	0.024	0.021	0.020	0.024	0.004	0.003	0.007
LOQ (µg/g brain tissue)	0.081	0.071	0.067	0.079	0.012	0.009	0.022
Mean curve R^2 (n = 5)	0.995	0.995	0.989	0.988	0.995	0.992	0.989

RSD = Relative square deviation; LOD = limit of detection; LOQ = limit of quantification

Table 4. Correlation analyses between Gb3 isoforms (normalized to brain weight) and α-Gal A activity, α-Gal A 46 kDa active species/Actin, or p129S-α-syn 17 kDa monomer/Actin.

	Correlation (Spearman r)		
Isoform (normalized to brain weight)	***α-Gal A activity***	***α-Gal A 46 kDa/Actin***	***α-syn p129S monomer/Actin***
C14:0	-0.3066, p=0.0340*	-0.245, p=0.0932	0.1611, p=0.2740
C16:0	-0.06389, p=0.6696	0.1247, p=0.4035	-0.255, p=0.0837
C18:0	-0.0906, p=0.5447	-0.01833, p=0.9027	-0.3197, p=0.0285*
C20:0	0.005699, p=0.9693	-0.2022, p=0.1681	0.1764, p=0.2305
C22:0	-0.2873, p=0.0477*	-0.4596, p=0.0010*	0.1908, p=0.1939
C24:0	-0.3598, p=0.0120*	-0.4344, p=0.0020*	0.307, p=0.0338*
C26:0	-0.3097, p=0.0.0322*	-0.1175, p=0.4264	0.3362, p=0.0195*
C16:1	0.02795, p=0.8504	-0.1604, p=0.2762	-0.1151, p=0.4361
C18:1	-0.1413, p=0.3434	-0.126, p=0.3989	-0.1893, p=0.2026
C20:1	-0.09299, p=0.5296	-0.04797, p=0.7461	-0.1162, p=0.4317
C22:1	-0.3409, p=0.0178*	-0.2959, p=0.0412*	0.1145, p=0.4384
C24:1	-0.2751, p=0.0584	-0.3075, p=0.0335*	0.02146, p=0.8849
C26:1	-0.3035, p=0.0360*	-0.1929, p=0.1889	0.4037, p=0.0044*
C22:2	-0.2233, p=0.1272	-0.1766, p=0.2299	0.1105, p=0.4547
C24:2	-0.2303, p=0.1154	-0.3213, p=0.0260*	0.03543, p=0.8111
C(16:0)OH	0.1511, p=0.3053	0.1515, p=0.3039	0.08367, p=0.5718
C(18:0)OH	-0.1864, p=0.2047	-0.1405, p=0.3410	0.3052, p=0.0349*
C(20:0)OH	-0.2564 p=0.0786	-0.169, p=0.2509	0.2553, p=0.0799
C(22:0)OH	-0.04855, p=0.7432	-0.2223, p=0.1288	0.1969, p=0.1797
C(24:0)OH	-0.3352, p=0.0199*	-0.3352, p=0.0199*	0.5028, p=00003*
C(22:1)OH	-0.0261, p=0.8602	-0.08735, p=0.5550	0.2111, p=0.1497
C(24:1)OH	-0.2239 p=0.1260	-0.2571, p=0.0777	0.1023, p=0.4889
C(16:0)Me	-0.3709, p=0.0094*	-0.2457, p=0.0923	0.01978, p=0.8938
C(18:0)Me	-0.01656, p=0.9110	-0.1558, p=0.2903	0.1091, p=0.4606
C(20:0)Me	-0.3089, p=0.0326*	-0.2905, p=0.0451*	0.3642, p=0.0109*
C(22:0)Me	-0.2353, p=0.1074	-0.3237, p=0.0248*	0.04717, p=0.7502
C(24:0)Me	-0.1975, p=0.1785	-0.2055, p=0.1612	0.3624, p=0.0114*
C(22:1)Me	0.1429, p=0.3326	-0.009977, p=0.9463	0.3725, p=0.0091*
C(24:1)Me	-0.05596, p=0.7056	-0.155, p=0.2929	0.02885, p=0.8457

Correlations were performed using non parametric Spearman's rho test and stepwise multiple linear regressions. * indicates significant correlations, with significance established *a priori* at p<0.05.

Table 5. Correlation analyses between Gb3 isoforms (normalized to brain sphingomyelin) with respect to α-Gal A activity, α-Gal A 46 kDa active species/Actin, and p129S-α-syn 17 kDa monomer/Actin.

	Correlation (Spearman r)		
Isoform (normalized to brain weight)	***α-Gal A activity***	***α-Gal A 46 kDa/Actin***	***α-syn p129S monomer/Actin***
C14:0	-0.3223, p=0.0250*	-0.2325, p=0.1118	0.4621, p=0.0009*
C16:0	-0.1958, p=0.1822	-0.004452, p=0.9760	-0.06465, p=0.6624
C18:0	-0.1287, p=0.3833	-0.1488, p=0.3128	-0.2271, p=0.1206
C20:0	-0.1008, p=0.4952*	-0.2034, p=0.1656	0.3563, p=0.0129*
C22:0	-0.313, p=0.0303*	-0.3829, p=0.0072*	0.3899, p=0.0062*
C24:0	-0.3507, p=0.0145*	-0.373, p=0.0090*	0.4215, p=0.0028*
C26:0	-0.351, p=0.0144*	-0.1688, p=0.2515	0.4242, p=0.0027*
C16:1	-0.2715, p=0.0619	-0.2041, p=0.1641	0.494, p=0.0004*
C18:1	-0.1969, p=0.1799	-0.2734, p=0.0601	-0.074, p=0.6172
C20:1	-0.2433, p=0.0956	-0.1501, p=0.3085	0.2087, p=0.1545
C22:1	-0.3714, p=0.0094*	-0.2981, p=0.0396*	0.3697, p=0.0097*
C24:1	-0.3503, p=0.0147*	-0.3746, p=0.0087*	0.2877, p=0.0474*
C26:1	-0.311, p=0.0314*	-0.193, p=0.1887	0.4268, p=0.0025*
C22:2	-0.2525, p=0.0834	-0.2303, p=0.1153	0.1812, p=0.2177
C24:2	-0.2904, p=0.0453*	-0.3877, p=0.0065*	0.2764, p=0.0572
C(16:0)OH	-0.005102, p=0.9725	0.08752, p=0.5542	0.3196, p=0.0268*
C(18:0)OH	-0.2042, p=0.1639	-0.1509, p=0.3061	0.3188, p=0.0272
C(20:0)OH	-0.2564, p=0.0786	-0.169, p=0.2509	0.2553, p=0.0799
C(22:0)OH	-0.1057, p=0.4745	-0.2118, p=0.1485	0.2461, p=0.0918
C(24:0)OH	-0.3431, p=0.0170*	-0.03436, p=0.8167	0.5172, p=0.0002*
C(22:1)OH	-0.04936, p=0.7390	-0.1135, p=0.4426	0.2474, p=0.0900
C(24:1)OH	-0.2224, p=0.1287	-0.09892, p=0.5036	0.2218, p=0.1297
C(16:0)Me	-0.3753, p=0.0086*	-0.3015, p=0.0373*	0.3438, p=0.0167*
C(18:0)Me	-0.003364, p=0.9819	-0.151, p=0.3057	-0.1193, p=0.4191
C(20:0)Me	-0.3206, p=0.0263*	-0.256, p=0.0791	0.461, p=0.0010*
C(22:0)Me	-0.2624, p=0.0716	-0.3783, p=0.0080*	0.09997, p=0.4990
C(24:0)Me	-0.2006, p=0.1715	-0.2064, p=0.1593	0.3649, p=0.0108*
C(22:1)Me	0.142, p=0.3356	-0.02286, p=0.8774	-0.3637, p=0.0111*
C(24:1)Me	-0.0749, p=0.6129	-0.1765, p=0.2301	0.04767, p=0.7477

Correlations were performed using non-parametric Spearman's rho test and stepwise multiple linear regressions. * indicates significant correlations, with significance established *a priori* at p<0.05.

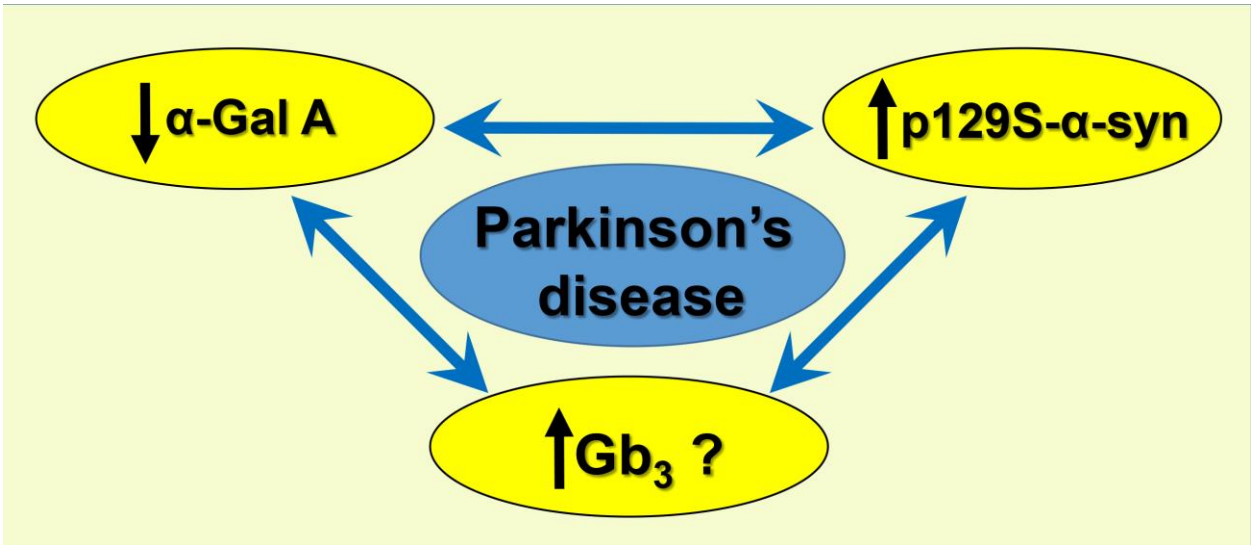

Graphical abstract

HIGHLIGHTS

- Significant reductions in alpha-Galactosidase A activity and protein were observed in late-stage Parkinson's disease temporal cortex
- Decreases in alpha-Galactosidase A and increases in several of its glycosphingolipid metabolites correlated significantly with the pathological increase in alpha-synuclein phosphorylated at serine 129
- These findings suggest the potential for alpha-Galactosidase A and its glycosphingolipid substrates as putative biomarkers and therapeutic targets for Parkinson's disease